CHAPTER VI

TRANSFER REACTIONS

1. INTRODUCTION

Transfer reactions have been of critical importance for the study of nuclear structure. The results obtained from the study of the stripping (d, p) and pickup (p, d) reactions involving single-neutron transfer helped to validate the nuclear shell model by identifying the single-particle states, since to a large extent the (d, p) reaction can be understood as one in which the neutron in the deuteron is transferred to a single-particle state of the final nucleus. In the pickup reaction, a neutron in a single-particle state is picked up by the incident proton to form the deuteron. Reactions in which a proton is transferred, such as the $(^3\text{He}, d)$ and $(d, ^3\text{He})$, provide similar information regarding the proton single-particle states. The reactions (t, p) and (p, t) involve the transfer of two neutrons. These reactions are most useful for study of the *superconducting* nuclei, such as the the tin isotopes. In these cases, the (t, p) reaction has a relatively large cross section for the transfer of two neutrons in the $^1S_0$ state, as predicted, for the formation of the final nucleus in a superconducting state.

In the course of these transfer reactions, energy, momentum, and angular momentum are exchanged by the projectile and target nucleus, as in the case for inelastic scattering. But in addition, in the transfer reaction there is a transfer of mass that produces a fundamental change in the description of the reaction from that used for inelastic scattering.

The strong specificity of these reactions at modest projectile energies follows from their surface character, a consequence of the limited penetration of the deuteron into the nuclear interior. If $\mathbf{p}_D$ is the incident deuteron momentum and $\mathbf{p}_f$ the momentum of the emerging proton, the momentum $\mathbf{p}_t$ transferred

to the target nucleus by the transfer of the neutron to the nucleus is given by conservation of momentum:

$$\mathbf{p}_t = \mathbf{p}_D - \mathbf{p}_f \tag{1.1}$$

From this equation one can immediately determine the magnitude of $\mathbf{p}_t$:

$$p_t^2 = p_D^2 + p_f^2 - 2p_D p_f \cos\vartheta \tag{1.2}$$

where ϑ is the angle between the direction of the final proton and the direction of the incident deuteron. The angular momentum transferred, $\hbar l_t$, must be less than $p_t R$, where R is the projectile–target separation at which the reaction occurs. Hence

$$\hbar^2(l_t + \tfrac{1}{2})^2 \leqslant p_t^2 R^2$$

or

$$(l_t + \tfrac{1}{2})^2 \leqslant (k_D^2 + k_f^2 - 2k_D k_f \cos\vartheta)R^2$$

so that

$$\cos\vartheta \leqslant \frac{(k_D R)^2 + (k_f R)^2 - (l_t + \frac{1}{2})^2}{2(k_D R)(k_f R)} \tag{1.3}$$

where $\hbar k$ as usual equals p, and the WKB value of $\hat{l}^2$, $(l + \frac{1}{2})^2$, has been used. Classically, then, one expects that the reaction will be forbidden for angles smaller than ϑ_m, the angle at which the equality of (1.3) is satisfied. Quantum mechanically, there will be some penetration into the classically forbidden region, so that the cross section should show a rise from $\vartheta = 0$ with a maximum at ϑ_m. One can employ that result to obtain an estimate of the value of l_t. R is treated as an empirical parameter, which, however, must be the same for all values of l_t.

For example, consider the $^{90}\mathrm{Zr}(d,p)^{91}\mathrm{Zr}$ reaction whose cross sections to various levels in $^{91}\mathrm{Zr}$ are given in Fig. 1.1. The similarity of the curves labeled $l = 2$ in the left-hand panel, of those labeled $l = 4$, and those labeled $l = 0$ is striking. If one assumes that the angle at the first peak equals ϑ_m, one can identify the l_t as well as R by requiring that R have a reasonable value. For example, the $l = 2$, $Q = 1.33$-MeV cross section gives $R = 5.4$ fm for $l_t = 2$, $R = 3.1$ fm for $l_t = 1$, and $R = 7.6$ fm for $l_t = 3$. When one takes into account the result obtained from quantitative studies that (1.3) underestimates the value of R at which the reaction occurs, the most reasonable value of R is 5.4 fm and the l_t transferred is 2. Using the same value of R, one can determine l_t for the three curves labeled $l = 4$ to be $l_t = 4$. The curves marked $l = 0$ have their first maxima at $\vartheta = 0$, which is presumed to be $l_t = 0$ transfer reaction.

The values $l_t = 0, 2, 4$ correspond very nicely to shell model expectations. The nucleus, $^{90}\mathrm{Zr}$, is a closed-shell nucleus [see Fig. IV.8.1 in deShalit and Feshbach

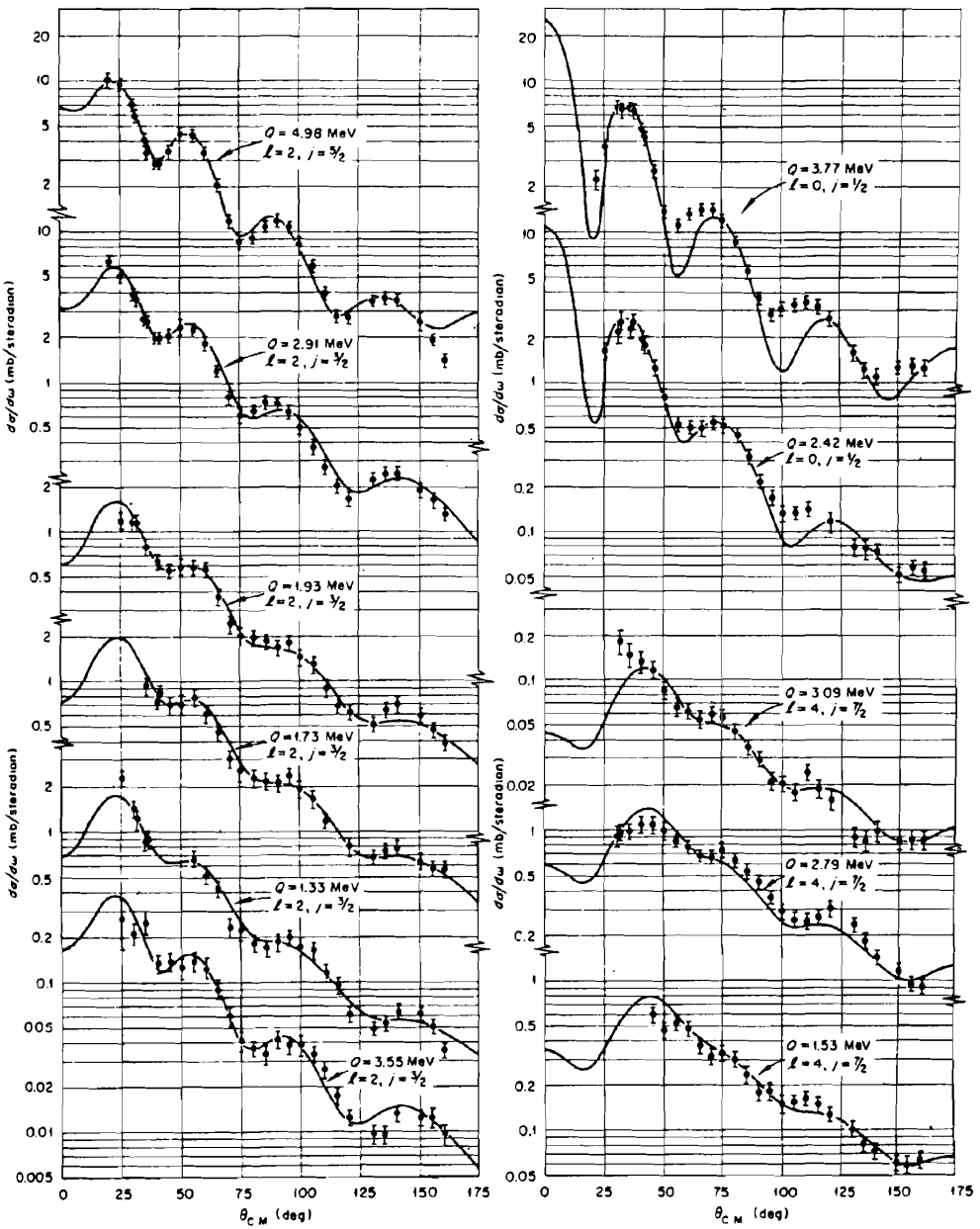

FIG. 1.1. Comparison between measurements and cross sections calculated using the distorted-waves method for the $^{90}Zr(d, p)$ ^{91}Zr reaction with 12-MeV deuterons. Transitions with $l = 0$, 2, and 4 are shown. [Dickens, Perey et al. (67)]. [From Satchler (83).]

(74)]. The neutron added in the (d,p) reaction would thus go into the shell, $50 \leqslant N \leqslant 82$ composed of $1g, 2d, 3s$ orbitals (i.e., $l = 4, 2, 0$), corresponding precisely to the values obtained for l_t.

The $^{90}Zr(d,p)$ example illustrates the extraordinary specificity of the (d,p) reaction that occurs at sufficiently low energies. By examining the angular distribution, one can deduce the orbital angular momentum transferred along with the captured neutron to the largest nucleus. Of course, a quantitative understanding of the angular distribution is essential before one can rely on this conclusion. The results of such a calculation, whose theoretical basis will be discussed later, are shown by the solid lines in Fig. 1.1. In this calculation it is assumed that the transferred neutron occupies a single-particle orbital of the target nucleus. The agreement with experiment is excellent (note the logarithmic scale for the cross sections)—an agreement with experiment that is repeated when targets throughout the periodic table are used, thus validating the single-step character of the transfer reaction mechanism.

The angular distribution is not sensitive[‡] to the value of the total angular momentum, j, transferred; that is, it does not distinguish between the two possible values, $j = l \pm \frac{1}{2}$. That sensitivity can be obtained in the (d,p) reaction using polarized deuterons and measuring the asymmetry of the produced protons. An example is shown in Fig. 1.2.

A qualitative understanding of the origin of the polarization of the proton emitted in (d,p) reaction (or equivalently, of the asymmetry of the emitted proton that occurs if the incident deuteron is polarized) has been given by Huby, Refai, and Satchler (58). For the production of nucleon polarization, it is essential that an asymmetry of the transition amplitude with respect to the normal to the scattering plane exist. The absence of such an asymmetry would make the production of a nucleon with a spin oriented in the "up" direction (i.e., in the direction of the normal to the scattering plane) indistinguishable from the production of a nucleon whose spin is in the opposite direction. An asymmetry will be present in the stripping amplitude for a given direction of the emergent proton if the amplitude differs according to which side of the target nucleus the stripping occurs. The origin of the asymmetry in the stripping amplitude lies classically in the differing paths, involving, for example, a different probability of absorption, taken by the proton and deuteron according to the side of the nucleus the deuteron strikes. Quantum mechanically, the asymmetry is a consequence of the distortion of the incident and emergent waves by the nuclear field. If the favored value of the projection, m, of the captured neutron is $(+l)$, and the spin of the final neutron single-particle state, j, is $l + \frac{1}{2}$, the neutron spin must be up. Since the incident spin of the deuteron is one, the spins of the neutron and proton are parallel, the emergent protons will be polarized with their spins up.

The determination of the spin-quantum numbers as well as of the energies

[‡]There does seem to be some dependence at back angles which is marked for $l = 1$, but less so for larger values of l [see Satchler (83, p. 706)].

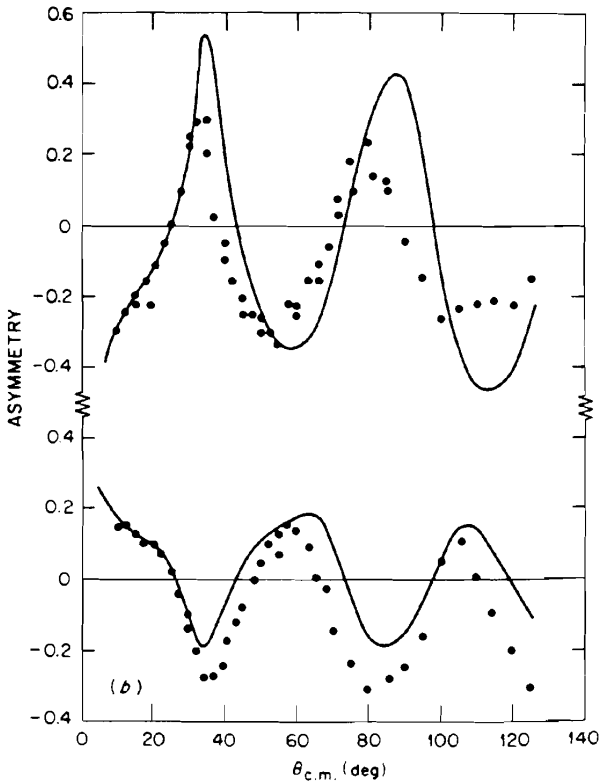

FIG. 1.2. Analyzing powers for $p_{1/2}$ (upper) and $p_{3/2}$ (lower) transfers in ^{52}Cr (**d**, p) reactions at 10 MeV. The curves are from DWA calculations [Kocher and Haberli (72)]. [From Satchler (1983).]

of the single-particle orbits provides obviously important spectroscopic information. But one can go beyond this to obtain information on the structure of the nuclear wave function. The single-particle orbit for the neutron provides only one component of the total wave function, which will, for example, include as well excitations of the target nucleus plus the neutron in other orbits. From the magnitude of the (d, p) cross section one can in principle determine the strength of the single-particle state generated by the (d, p) reaction. More precisely, the single-particle component of the final-state wave function has the form

$$\frac{1}{\sqrt{A+1}}\mathscr{A}[\Psi_T(1, 2, \ldots, A)\phi_{jm}(A+1)] \tag{1.4}$$

where $\mathscr{A}$ is the antisymmetry operator, Ψ_T the target nucleus wave function, and ϕ_{jm} the single-particle wave function. The quantity $\mathscr{S}(j)$, referred to as the

spectroscopic factor, measures the strength of the single-particle component in the final-state wave function, so that

$$\mathscr{S}^{1/2}(j) = \frac{1}{\sqrt{A+1}} \langle \mathscr{A}[\Psi_T(1,2,\ldots,A)\phi_{jm}(A+1)] | \Psi_f(1,2,\ldots,A,A+1) \rangle \quad (1.5)$$

and

$$\Psi_f = \frac{\mathscr{S}^{1/2}}{\sqrt{A+1}} \mathscr{A}(\Psi_T \phi_{jm}) + \cdots$$

$\mathscr{S}(j)$ is unity only in the limit of the noninteracting independent particle shell model for closed-shell target nuclei. This result holds not only for (d, p) reactions but also for (p, d) reaction. In the later, instead of adding a particle to the closed-shell target, one creates a "hole" in a filled shell. This is made completely clear in a formalism in which particle and hole formation are treated symmetrically, as described in (VII.9.11) in deShalit and Feshbach (74). However, in the interacting shell model any state of the $A + 1$ system will consist of a linear combination of one-particle states and two-particle/one-hole states, three-particle/two-hole states, and so on. In that case $\mathscr{S}_j$ will be less than 1; the deviation from one describing the probability that the system is not in a single-particle state given by (1.4).

Can the spectroscopic factor be determined experimentally? The answer is that any such determination is model dependent. To be sure, the cross section is proportional to $\mathscr{S}_j$. But the other factors depend on the models used for describing the initial and final wave functions as well as upon the interactions of the proton and neutron with the target nucleus as well as their mutual interaction. Only if these are well known can $\mathscr{S}_j$ be determined from the magnitude of the cross section. Within a given framework, that is, a particular nuclear model and fixed interactions, the relative value of $\mathscr{S}_j$ are meaningful, especially if a consistent picture of the reaction over a range of nuclei can be established.

Consistency must also be established with respect to other models of populating single-particle states. One obvious example is the (n, γ) reaction, in which the neutron after γ emission ends up in the same state produced in the (d, p) reaction. Another example is the isobar analog resonance. For example, through the resonant elastic scattering of protons on an (N, Z) nucleus, one obtains information on the analog states in the $(N + 1, Z)$ nucleus [see deShalit

FIG. 1.3. Angular distributions for nucleon transfer at sub-Coulomb energies for different l transfers. The curves are the results of DWA calculations: (*a*) (d, p) at 8.0 MeV [Erskine, Buechner and Enge et al. (62)]; (*b*) (^{17}O, ^{16}O) reaction at 67 MeV [Franey Lilley and Phillips et al. (79)]. [From Satchler (83).]

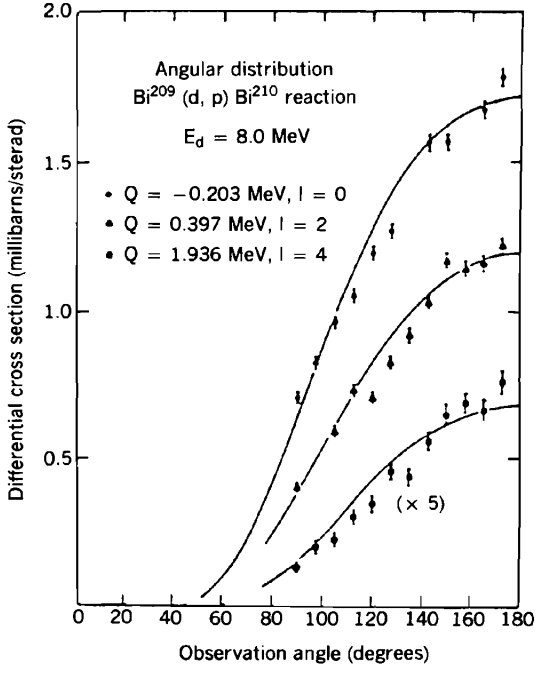
Angular distribution
Bi209 (d, p) Bi210 reaction
Ed = 8.0 MeV
• Q = −0.203 MeV, l = 0
• Q = 0.397 MeV, l = 2
• Q = 1.936 MeV, l = 4
(× 5)
Differential cross section (millibarns/sterad)
Observation angle (degrees)
2.0
1.5
1.0
0.5
0
20
40
60
80
100
120
140
160
180

(a)

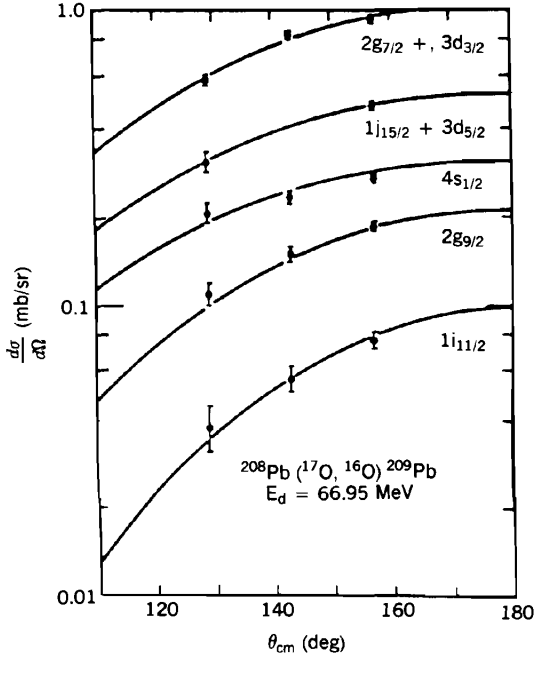
2g7/2 +, 3d3/2
1j15/2 + 3d5/2
4s1/2
2g9/2
1i11/2
208Pb (17O, 16O) 209Pb
Ed = 66.95 MeV
dσ/dΩ (mb/sr)
θcm (deg)
1.0
0.1
0.01
120
140
160
180

and Feshbach (74, p. 102)], which again can be compared with the (d, p) reaction on the target (N, Z) nucleus.

The striking correlation between the (d, p) angular distribution and nuclear structure is present only in a limited energy range. At very low energies, below the Coulomb barrier, the process is dominated by the Coulomb interaction and the angular distributions are rather featureless (Fig. 1.3). At high energies, the

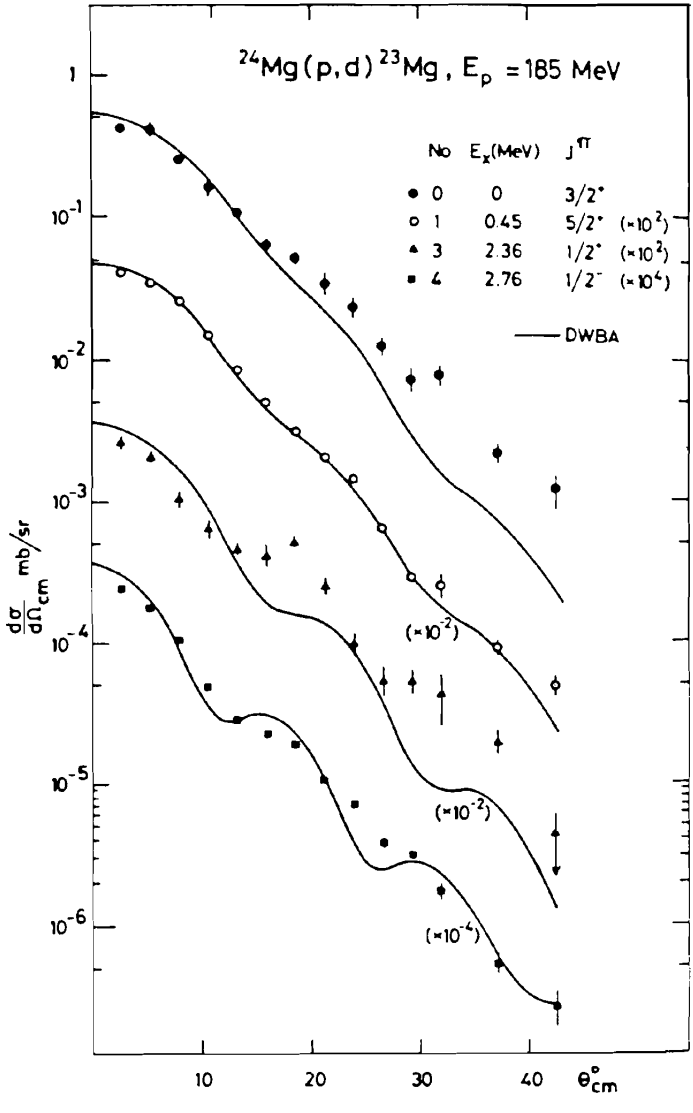

FIG. 1.4. Angular distributions for medium-energy (p, d) reactions. The curves are from DWA calculations [Kallne and Fagerstrom (79)]. [From Satchler (83).]

deuteron penetrates into the nuclear interior, and again the angular distribution does not as directly provide nuclear structure information (Fig. 1.4). It is the intermediate energy region throughout which the deuteron can penetrate to the nuclear surface, but not much beyond, that (d,p) experiments manifest their, specificity most clearly. The reaction in this energy domain is peripheral and it is this condition that underlies the interpretation of the resulting structured angular distribution.

2. THE DWA AMPLITUDE

For the most part, the analysis of the (d,p) and (p,d) reactions has been based on the distorted wave approximation (DWA). Its derivation is, however, not as straightforward as the DWA for inelastic scattering given in Chapter V. In that case the DWA amplitude is an approximation to the solution of a pair of coupled equations obtained by projecting out the incident and inelastic channels. The effect of the remaining channels was included through an energy averaging that introduced imaginary components into both the diagonal and coupling potentials. An important element in this procedure is the orthogonality of the ground state and the excited state of the target nucleus. To be sure, when the incident particle is a nucleon or composed of nucleons, this advantage is diluted by the nonorthogonality introduced by the Pauli principle, but we have learned how to take account of that feature by the method developed in Section III.5.

Extension to the case of particle transfer is possible, but there is a characteristic problem that must first be resolved. To be concrete, let us consider the $^{16}O(d,p)^{17}O$ stripping reaction. In that case one must consider at least the two partitions [Satchler (83)] $d + {}^{16}O$ and $p + {}^{17}O$ of the 18-particle system. The natural spatial coordinates of the first partition include the relative distance between the neutron and proton of the deuteron and the distance between the center of mass of the deuteron and the center of mass of the ^{16}O nucleus, and finally, the (3×15) independent internal coordinates of the nucleons making up the ^{16}O nucleus. The total number of coordinates should be (3×17). However, these coordinates are not convenient for the description of the final system, which involves the distance between the proton and the center of mass of the ^{17}O nucleus and the (3×16) independent internal coordinates for the ^{17}O nucleus. It is possible to introduce a complete set of the $d + {}^{16}O$ wave functions that would need to include the continuum states of the deuteron, in which the neutron and proton are no longer bound in order to include a description of the final state, $p + {}^{17}O$.

Diagrammatically (Fig. 2.1), the deuteron breaks up at vertex 1, the proton moving ahead while the released neutron is captured by the ^{16}O nucleus to form ^{17}O. Diagrams of this sort and their corresponding analytic transition amplitudes are very helpful for forming an intuitional understanding and have provided the base for theories developed by Shapiro (67) and Schnitzer (64).

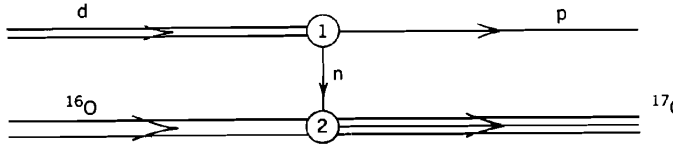

FIG. 2.1. Stripping reaction.

However, they have not for the most part been adopted as the preferred method for analyzing particle transfer reactions.

The method, which is most commonly used and which by suitable manipulations leads to the DWA, employs a mixed representation. In the initial channel, this might include the deuteron and ^{16}O in their ground state plus excited states of ^{16}O. In the final channel one would include the proton plus various states of ^{17}O according to the reaction involved. The total wave function would then contain contributions from both of these sets of wave functions. The remainder will be energy averaged with the consequent introduction of complex potentials. Such a wave function would permit the calculation of not only the one-step process but also for the multistep process, of which the two-step is illustrated in Fig. 2.2. The wave function corresponding to that figure would include the ^{16}O and ^{17}O ground and first excited states.

A traditional approach to the *single-step process* [say, (d,p)] has been to truncate the wave function Ψ of the system as follows:

$$\Psi = \mathscr{A}[u\phi + v\chi\psi] + \cdots \tag{2.1}$$

where ϕ is the residual nucleus wave function (^{17}O), χ the internal deuteron wave function, and ψ the initial nucleus wave function. The functions u (proton) and v (deuteron) to be determined depend on the distance between the proton and center of mass of ^{17}O, the residual nucleus, and between the center of mass of the deuteron and ^{16}O, the initial nucleus, respectively. $\mathscr{A}$ is the antisymmetrization operator. The indicated truncation does have a serious drawback. The omitted terms in the series would contain components such as excited

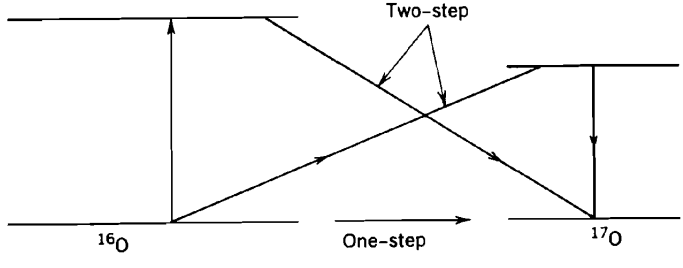

FIG. 2.2. One- and two-step contributions to a pickup reaction.

states of ^{17}O, which together with the proton wave function would have a substantial overlap with the deuteron channel wave function $\chi\psi$. It therefore should be included in (2.1) in order to obtain the total asymptotic reaction amplitude. Similarly, excited continuum states of the deuteron combined with the ^{16}O wave wave function (ground and excited states) would combine to form $^{17}O + p$ states. These difficulties are very similar to that of exchange scattering discussed in Section III.5 and are resolved in exactly the same way. We write

$$\Psi = P\Psi + Q\Psi \tag{2.2}$$

where as usual P and Q are projection operators and $Q = 1 - P$. $P\Psi$ is

$$P\Psi = \mathscr{A}[u\phi + v\chi\psi] \tag{2.3}$$

Because

$$\langle P\Psi | Q\Psi \rangle = 0 \tag{2.4}$$

and the related constraints

$$\langle \phi | Q\Psi \rangle = 0 \tag{2.5}$$

$$\langle \chi\psi | Q\Psi \rangle = 0 \tag{2.6}$$

$Q\Psi$ will not contain any components that can contribute to $u\phi$ or $v\chi\psi$. The function $P\Psi$ contains all the information required for the determination of the reaction amplitude. Conditions (2.5) and (2.6) also solve the problems raised by the identity of the particles involved. The reasoning is identical with that given in Section III.5 and need not be repeated.

Before proceeding to a consideration of (2.5) and (2.6), it is useful to point to another problem associated with ansatz [see (2.1)]. This can be seen if one substitutes $u\phi + v\chi\psi$ for Ψ in the Schrödinger equation

$$H\Psi = E\Psi \tag{2.7}$$

We drop the antisymmetrization operator, $\mathscr{A}$, to simplify the argument. Including $\mathscr{A}$ will not change the substance of the discussion. Multiplying (2.7) from the left by ϕ and integrating over all the coordinates contained in ϕ yields an equation for u coupled to v. A second equation is obtained by multiplying by $\chi\phi$ and integrating. These equations are

$$\langle \phi | Hu\phi \rangle - Eu = E\langle \phi | v\chi\psi \rangle - \langle \phi | Hv\chi\psi \rangle \tag{2.8a}$$

$$\langle \chi\psi | Hv\chi\psi \rangle - Ev = E\langle \chi\psi | u\phi \rangle - \langle \chi\psi | Uu\phi \rangle \tag{2.8b}$$

We observe the presence of a coupling term on the right-hand side of each of these equations, proportional to the energy. These are present because ϕ is not

orthogonal to $\chi\psi$. The range of this coupling term is given roughly by the radius of the deuteron, which is relatively large. Some study of this situation has been made. [See Satchler (83), Section 3.32, for further discussion; see also Ohmura, Imanishi, Schimura, and Kawai (70); Imanishi et al (74); Cotanch (75); and Cotanch and Vincent (76).] Satchler summarizes by noting that in the cases discussed by these authors "the effects [of these terms] appears to be small, not always negligible on the absolute sense, but with the uncertainties that one might subjectively associate with the models being used." In the standard DWA applications, these overlap terms are generally ignored. As we shall show, terms of this type (proportional to the energy E) need not appear in the coupled equations for u and v when the representation (2.2)–(2.6) is used.

These equations are exact. However, the choice for $P\Psi$, and the eventual replacement of $Q\Psi$ by an energy average introducing thereby an optical potential into the equation for $P\Psi$, involve some implicit assumptions. The possibilities not explicitly included in (2.3), such as multistep processes as well as the polarization of the deuteron under the combined influence of electrostatic and nuclear fields, are assumed either to be of little importance or to have effects that vary slowly with the experimental parameters. Under the latter set of circumstances it may be expected that a correspondingly slow variation in the optical model parameters determined empirically will suffice to take these effects into account.

We turn now to (2.2)–(2.6). A complete analysis of these equations has been given by Döhnert (68, 71) [see also Mittelman (64), and Horiuchi (77)]. Formally, the results are quite simple. However, Döhnert's calculations are quite complicated, although with the computational aids developed since that paper appeared they should be much less formidable. In the present context, Döhnert's results are important since they demonstrate the existence of the projection operator P and therefore of coupled equations for u and v from which the DWA can be extracted. Note that the results to be obtained below apply, after suitable but trivial generalizations, to the collision of a heavy ion with a nucleus.

Equations (2.5) and (2.6) reduce to two equations for u and v in terms of U and V defined by

$$U \equiv \langle \phi | \Psi \rangle \qquad V \equiv \langle \chi\psi | \Psi \rangle \tag{2.9}$$

where the integrations are carried out only over the variables in ϕ and $\chi\psi$, respectively. Consider first (2.5):

$$0 = \langle \phi | Q\Psi \rangle = \langle \phi | \Psi \rangle - \langle \phi | P\Psi \rangle \tag{2.10}$$

We immediately obtain

$$U = \langle \phi | P\Psi \rangle \tag{2.11}$$

and similarly,

$$V = \langle \chi\psi | P\Psi \rangle \tag{2.12}$$

Substituting (2.3) in (2.10), one obtains

$$U = \langle \phi | \mathscr{A}(u\phi) \rangle + \langle \phi | \mathscr{A}(v\chi\psi) \rangle$$

Defining the operators K_{uu} and K_{uv} by

$$(1 - K_{uu})u \equiv \langle \phi | \mathscr{A}(u\phi) \rangle \qquad K_{uv}v \equiv -\langle \phi | \mathscr{A}(v\chi\psi) \rangle \tag{2.13}$$

the equation for U becomes

$$U = (1 - K_{uu})u - K_{uv}v \tag{2.14}$$

Note that operator K_{uu} [identical with K of (III.5.13)] is Hermitian. This can be seen formally since the operator

$$1 - K_{uu} \equiv \langle \phi | \mathscr{A}\phi \rangle = \langle \mathscr{A}\phi | \phi \rangle \tag{2.15}$$

A similar analysis of (2.6) yields

$$V = (1 - K_{vv})v - K_{vu}^{\dagger}u \tag{2.16}$$

where K_{vv} is Hermitian since

$$1 - K_{vv} = \langle \chi\psi | \mathscr{A}\chi\psi \rangle = \langle \mathscr{A}\chi\psi | \chi\psi \rangle$$

The operator K_{uu} and K_{uv} contain the effects of antisymmetry while the nondiagonal K_{uv} includes the antisymmetry and overlap effects. Defining

$$W \equiv \begin{pmatrix} U \\ V \end{pmatrix} \qquad w \equiv \begin{pmatrix} u \\ v \end{pmatrix} \qquad \hat{K} \equiv \begin{pmatrix} K_{uu} & K_{uv} \\ K_{vu}^{\dagger} & K_{vv} \end{pmatrix} \tag{2.17}$$

Equations (2.13) and (2.16) can be summarized as follows:

$$W = (1 - \hat{K})w \tag{2.18}$$

where $\hat{K}$ is Hermitian. This equation is identical in form with (III.5.15) and its analysis is completely parallel to that following this equation.

Since $\hat{K}$ is Hermitian its eigenvalues κ_α are real and its eigenfunctions w_α forms an orthonormal set. Moreover, $(1 - \hat{K})$ is positive definite. To prove this, note that

$$\langle w | (1 - \hat{K})w \rangle = \langle u\phi + v\chi\psi | \mathscr{A}(u\phi + v\chi\psi) \rangle \tag{2.19}$$

Because of the antisymmetry of the ket, this can be written as

$$\langle \mathscr{A}(u\phi + v\chi\psi) | \mathscr{A}(u\phi + v\chi\psi) \rangle \geqslant 0 \tag{2.20}$$

We can additionally conclude that the eigenvalues of $\hat{K}$, κ_α, are less than 1:

$$\kappa_\alpha \leqslant 1 \tag{2.21}$$

Since the operators in $\hat{K}$ involve only square-integrable functions [see (2.13) and (2.15)], $\hat{K}$ is bounded. The trace of $\hat{K}$, tr $\hat{K}$, involves the trace of K_{uu} and K_{vv} only. These traces have been shown to be bounded in the discussion dealing with elastic scattering, so that tr $\hat{K}$ is bounded. We can therefore conclude that the eigenvalue spectrum of $\hat{K}$ is discrete.

Special attention needs to be paid to $w_\alpha^{(1)} = \begin{pmatrix} u_\alpha^{(1)} \\ v_\alpha^{(1)} \end{pmatrix}$, eigenfunctions of $\hat{K}$ whose eigenvalue κ_α is unity $\hat{K}w_\alpha^{(1)} = w_\alpha^{(1)}$. We shall show that

$$\mathscr{A}(u_\alpha^{(1)}\phi + v_\alpha^{(1)}\chi\psi) \equiv 0 \tag{2.22}$$

To prove this, note that

$$\langle \mathscr{A}(u\phi + v\chi\psi) | \mathscr{A}(u\phi + v\chi\psi) \rangle = \langle (1 - \hat{K})w | (1 - \hat{K})w \rangle$$

Inserting $w_\alpha^{(1)}$ for w in this last equation, we obtain

$$\langle \mathscr{A}(u_\alpha^{(1)}\phi + v_\alpha^{(1)}\chi\psi) | \mathscr{A}(u_\alpha^{(1)}\psi + v_\alpha^{(1)}\chi\psi) \rangle = \langle (1 - \hat{K})w_\alpha^{(1)} | (1 - \hat{K})w_\alpha^{(1)} \rangle = 0$$

Equation (2.22) follows from this result. These solutions, $w_\alpha^{(1)}$, are referred to as *superfluous solutions* [see (III.5.19)]. These solutions do not contribute to $P\Psi$, as follows from (2.22).

These results are for the most part similar to the results obtained for elastic and inelastic scattering with one notable difference. In elastic and inelastic scattering the appearance of K and the associated superfluous solutions are formally a consequence of the nonorthogonality introduced by antisymmetrization. In the particle transfer case, $\hat{K}$ and the associated superfluous solutions arise not only because of antisymmetrization but also because of the overlap between the cluster wave functions ϕ and $\chi\psi$.

We are now able to invert (2.18):

$$w = \frac{1}{1 - \hat{K}'} W \tag{2.23}$$

where the prime superscript on $\hat{K}'$ indicates that in the spectral expansion of $\hat{K}'$,

$$\hat{K}' = \sum_{\kappa_\alpha \neq 1} \kappa_\alpha w_\alpha \rangle\langle w_\alpha \tag{2.24}$$

all eigenfunctions of $\hat{K}$ with unit eigenvalue are to be omitted. Hence

$$w = \sum_{\kappa_\alpha \neq 1} \frac{1}{1 - \kappa_\alpha} w_\alpha \rangle\langle w_\alpha | W \rangle = W + \sum_{\kappa_\alpha \neq 1} \frac{\kappa_\alpha}{1 - \kappa_\alpha} w_\alpha \rangle\langle w_\alpha | W \rangle$$

An explicit expression for the projection operator P of (2.3) can be obtained. Define matrices $\Phi\rangle$ and $\langle\Phi$ as follows:

$$\Phi\rangle \equiv \begin{pmatrix} \phi \\ \chi\psi \end{pmatrix} \qquad \langle\Phi \equiv (\phi, \chi\psi) \tag{2.25}$$

Equation (2.3) can then be written

$$P\Psi = \mathscr{A}(\Phi, w) = \mathscr{A}(\phi, \chi\psi)\begin{pmatrix} u \\ v \end{pmatrix} = \mathscr{A}(u\phi + v\chi\psi)$$

Inserting (2.23) and noting that the matrix W is

$$W = \begin{pmatrix} \langle\phi|\Psi\rangle \\ \langle\chi\psi|\Psi\rangle \end{pmatrix} = \langle\Phi|\Psi\rangle \tag{2.26}$$

we have

$$P = \mathscr{A}\Phi\rangle \frac{1}{1-\hat{K}'}\langle\Phi \tag{2.27}$$

Employing the spectral series for $1/(1-\hat{K}')$ with

$$w_\alpha = \begin{pmatrix} u_\alpha \\ v_\alpha \end{pmatrix}$$

one obtains

$$P = \sum_{\kappa_\alpha \neq 1} \mathscr{A}\left[u_\alpha\phi + v_\alpha\chi\psi\rangle \frac{1}{1-\kappa_\alpha}\langle u_\alpha\phi + v_\alpha\chi\psi \right]$$

Once P is known it becomes possible to obtain the Schrödinger equation for $P\Psi$ and the coupled system for u and v. The constraints on u and v are now carried by the operator $(1/1-\hat{K}')$. The equation for $P\Psi$, (III.2.7), is

$$\left(E - H_{PP} - H_{PQ}\frac{1}{E-H_{QQ}}H_{QP}\right)P\Psi = 0 \tag{III.2.7}$$

Upon energy averaging, the last two terms can be combined into a complex (i.e., non-Hermitian) optical model Hamiltonian, $PH_{\text{eff}}P$:

$$(E - PH_{\text{eff}}P)P\Psi = 0 \tag{2.28}$$

Multiplying from the left by Φ and integrating, one obtains

$$EW = \langle \Phi | P H_{\text{eff}} P \Psi \rangle = \langle \Phi | H_{\text{eff}} P \Psi \rangle \tag{2.29}$$

and from (2.27),

$$\begin{aligned} EW &= \left\langle \Phi | H_{\text{eff}} \mathscr{A} \Phi \frac{1}{1-\hat{K}'} W \right\rangle \\ &= \langle \Phi | H_{\text{eff}} \mathscr{A} \Phi w \rangle = \langle \Phi | H_{\text{eff}} \mathscr{A} (u\phi + v\chi\psi) \rangle \end{aligned} \tag{2.30}$$

an equation determining W [see (2.17) and (2.26)]. Note that the operator $\langle \Phi | \mathscr{A} \Phi (1/1-\hat{K}')$ is just the unit operator since $\langle \Phi | \mathscr{A} \Phi \rangle$ equals $(1-\hat{K})$. Therefore, (2.29) can also be written

$$\left\langle \Phi | (E - H_{\text{eff}}) \mathscr{A} \Phi \frac{1}{1-\hat{K}'} W \right\rangle = 0 \tag{2.31}$$

This is a pair of coupled equations for U and V:

$$\begin{aligned} &EU - \left\langle \phi | H_{\text{eff}} \mathscr{A} \left\{ \phi \left[\frac{1}{1-\hat{K}'} \right]_{uu} + \chi\psi \left[\frac{1}{1-\hat{K}'} \right]_{vu} \right\} U \right\rangle \\ &\quad = - \left\langle \phi | (E - H_{\text{eff}}) \mathscr{A} \left\{ \phi \left[\frac{1}{1-\hat{K}'} \right]_{uv} + \chi\psi \left[\frac{1}{1-\hat{K}'} \right]_{vv} \right\} V \right\rangle \end{aligned} \tag{2.32a}$$

$$\begin{aligned} &EV - \left\langle \chi\psi | H_{\text{eff}} \mathscr{A} \left\{ \phi \left[\frac{1}{1-\hat{K}'} \right]_{uv} + \chi\psi \left[\frac{1}{1-\hat{K}'} \right]_{vv} \right\} V \right\rangle \\ &\quad = - \left\langle \chi\psi | (E - H_{\text{eff}}) \mathscr{A} \left\{ \phi \left[\frac{1}{1-\hat{K}'} \right]_{uu} + \chi\psi \left[\frac{1}{1-\hat{K}'} \right]_{vu} \right\} U \right\rangle \end{aligned} \tag{2.32b}$$

One can immediately obtain the transition amplitude for the (d, p) reaction from (2.32a):

$$\mathscr{T}_{dp} = - \left\langle U^{(-)}_{0,f} \phi | (E - H_{\text{eff}}) \mathscr{A} \left\{ \left(\phi \left[\frac{1}{1-\hat{K}'} \right]_{uv} + \chi\psi \left[\frac{1}{1-\hat{K}'} \right]_{vv} \right) V^{(+)}_i \right\} \right\rangle \tag{2.33}$$

where $U_{0,f}$ satisfies the homogeneous equation (2.32a):

$$EU_0 = \left\langle \phi | H_{\text{eff}} \mathscr{A} \left\{ \phi \left[\frac{1}{1-\hat{K}'} \right]_{uu} + \chi\psi \left[\frac{1}{1-\hat{K}'} \right]_{vu} \right\} U_0 \right\rangle \tag{2.34}$$

The quantity $U_{0,f}\phi$ describes the elastic channel proton-residual nucleus wave function, taking into account the orthogonality to the deuteron–target nucleus channel but omitting the coupling to that channel, that is, to V. It therefore satisfies a Schrödinger equation involving just the Hamiltonian, H_f, describing the effective interaction in the elastic final-state channel:

$$H_f(U_{0,f}\phi) = E(U_{0,f}\phi) \tag{2.35}$$

The residual interaction giving the coupling to the deuteron channel is

$$\mathscr{V}^{(f)} \equiv H_{\text{eff}} - H_f \tag{2.36}$$

Therefore,

$$\mathscr{T}_{dp} = \left\langle U_{0,f}^{(-)}\phi \middle| \mathscr{V}^{(f)}\mathscr{A}\left\{\phi\left[\frac{1}{1-\hat{K}'}\right]_{uv} + \chi\psi\left[\frac{1}{1-\hat{K}'}\right]_{vv}\right\} V_i^{(+)}\right\rangle \tag{2.37}$$

With this equation we obtain a complete formal solution of the particle transfer problem, including the effects of nonorthogonality and antisymmetry. Its derivation is sufficiently general so that it can be applied to any transfer reaction (e.g., those induced by heavy ions) for which (2.3) is appropriate and can readily be generalized to other cases, since the structure given by (2.18) of the relation between W and w and the Schrödinger equation for $P\Psi$, (III.5.26) remains unchanged.

Problem. Define

$$\bar{W} \equiv \frac{1}{\sqrt{1-\hat{K}'}} W \tag{2.38}$$

Show that

$$E\bar{W} = \left\langle \Phi \middle| \frac{1}{\sqrt{1-\hat{K}'}} H_{\text{eff}}\mathscr{A}\Phi \frac{1}{\sqrt{1-\hat{K}'}} \bar{W}\right\rangle \tag{2.39}$$

In this equation, the operator acting on W on the right-hand side is symmetric, implying time-reversal invariance.

A number of approximations are commonly applied to (2.37). Many authors neglect the nonorthogonality kernels K_{uv} and $K_{uv}^{\dagger}$ [Eq. (2.13)]. $\hat{K}$ is then diagonal, with the consequence that only the effects of antisymmetry in the initial and final channels are taken into account. For example, (2.34) for U_0 becomes

$$EU_0 \simeq \left\langle \phi \middle| H_{\text{eff}}\left(\frac{1}{1-K'_{uu}}\right) U_0\right\rangle \tag{2.40}$$

which is just the equation satisfied by the wave function for proton scattering by the residual nucleus. Since H_{eff} is determined empirically, some of the coupling and orthogonality effects are included. Similarly, (2.32) for U simplifies to

$$EU - \left\langle \phi | H_{\text{eff}} \mathscr{A} \left\{ \phi \frac{1}{1 - K'_{uu}} U \right\} \right\rangle = - \left\langle \phi | (E - H_{\text{eff}}) \mathscr{A} \left\{ \chi\psi \frac{1}{1 - K'_{vv}} V \right\} \right\rangle$$

or

$$EU - \langle \phi | H_{\text{eff}} \mathscr{A}(\phi u) \rangle = - \langle \phi | (E - H_{\text{eff}}) \mathscr{A}(v\chi\psi) \rangle \tag{2.41}$$

The equation for V becomes

$$EV - \left\langle \chi\psi | H_{\text{eff}} \mathscr{A} \left\{ \chi\psi \frac{1}{1 - K'_{vv}} \right\} V \right\rangle = - \left\langle \chi\psi | (E - H_{\text{eff}}) \mathscr{A} \left\{ \phi \frac{1}{1 - K'_{uu}} U \right\} \right\rangle$$

or

$$EV - \langle \chi\psi | H_{\text{eff}} \mathscr{A}(v\chi\psi) \rangle = - \langle \chi\psi | (E - H_{\text{eff}}) \mathscr{A}(u\phi) \rangle \tag{2.42}$$

The transition matrix equation (2.37) reduces to

$$\mathscr{T}_{dp} \simeq \left\langle U^{(-)}_{0,f} \phi | \mathscr{V}^{(f)} \mathscr{A} \left\{ \chi\psi \left(\frac{1}{1 - \hat{K}'} \right)_{vv} V^{(+)}_i \right\} \right\rangle \tag{2.43}$$

$$= \langle U^{(-)}_{0,f} \phi | \mathscr{V}^{(f)} \mathscr{A}(v^{(+)}_i \chi\psi) \rangle \tag{2.44}$$

where U_0 now satisfies (2.40). Finally, the approximation in which $V^{(+)}_i$ in (2.43) is replaced by the "unperturbed" $V^{(+)}_{0,i}$, which satisfies

$$EV_0 - \left\langle \chi\psi | H_{\text{eff}} \mathscr{A} \left\{ \chi\psi \frac{1}{1 - K'_{vv}} V_0 \right\} \right\rangle = 0 \tag{2.45}$$

is made. One obtains

$$\mathscr{T}^{(\text{DWA})}_{dp} = \left\langle U^{(-)}_{0,f} \phi | \mathscr{V}^{(f)} \mathscr{A} \left\{ \left(\frac{1}{1 - K'_{vv}} \right)_v V^{(+)}_{0,i} \right\} \right\rangle \tag{2.46}$$

or the more familiar form

$$\mathscr{T}^{(\text{DWA})}_{dp} = \langle U^{(-)}_{0,f} \phi | \mathscr{V}^{(f)} \mathscr{A}(v^{(+)}_{0,i} \chi\psi) \rangle \tag{2.46'}$$

As has been pointed out earlier, much of the error of the last approximation may be reduced because of the use of an empirical interaction for $\mathscr{V}^{(f)}$. In

principle, one could eliminate V from (2.41) by first solving (2.42) for V in terms of W and substituting in (2.41). The effects of antisymmetrization as required in (2.46) or (2.43) can be carried out by direct evaluation of the eigenfunctions and eigenvalues of the operator $\hat{K}_{vv}$. These can be used to provide a representation of $1/(1-K'_{vv})$. Another procedure requires finding only the eigenfunction of the operator K_{vv}, $V_\alpha^{(1)}$, with eigenvalue of unity and then insisting that $v_{0,i}$ be orthogonal to all the $v_\alpha^{(1)}$ [Saito (68, 69)]. For a review of recently developed procedures, see Arima (78) and Horiuchi (77). A recent example is in the paper by Kato, Okabe, and Abe (85). Of course, there may be circumstances in which the non-orthogonality operator K_{uv} cannot be neglected (much here depends on the choice for ϕ and $\chi\psi$). In that event one must return to the exact $\mathscr{T}_{dp}$ of (2.37). The DWA result would then be obtained by replacing $V_i^{(+)}$ by $V_{0,i}^{(+)}$ in that equation.

In principle, the application of (2.46) is straightforward. One must first obtain the elastic channel wave functions for the deuteron–target nucleus and the proton–residual nucleus systems with appropriate attention to the requirements of antisymmetry. These wave functions are solutions of a Schrödinger-type equation [see (2.45) and (2.40)]. Since we are considering a prompt process, H_{eff} is taken to be an optical model complex Hamiltonian, while H_f is the diagonal part of H_{eff} in the (p-nucleus) channels, and $\mathscr{V}^{(f)}$ is the nondiagonal part. Note that one must be careful to maintain the permutation symmetry of the underlying Hamiltonian in choosing $\mathscr{V}^{(f)}$. A simple procedure is to antisymmetrize $U_{0,f}^{(-)}$ before inserting $\mathscr{V}^{(f)}$ and multiply by $1/A+1$, where $A+1$ is the total number of nucleons.

In actual practice, the elastic channel wave function is obtained as a solution of the single-channel optical model Hamiltonian which has been adjusted so that the resulting elastic scattering cross sections agree with experiment. Usually, these wave functions do not satisfy the Pauli exclusion principle so that its effect must in some fashion and to some extent be contained in the empirical potential used.This is more explicit when the potential is a folded one, as antisymmetry gives rise to an exchange term. One is in serious danger of overcounting if one simply orthogonalizes the empirical wave functions with respect to $\chi\psi v_\alpha^{(1)}$ [Fleissbach and Mang (76); Fleissbach (78)]. One should obviously return to the original elastic scattering problem and readjust the optical potential so that orthogonality with respect to the superfluous solutions and agreement with the experimental data are obtained simultaneously.

Post-prior Representations. Equation (2.33) for $\mathscr{T}$ can be condensed by staying with the Φ, W formalism [see (2.26)]. It becomes

$$\begin{aligned}\hat{\mathscr{T}}_{fi} &= \langle W_{0,f}^{(-)}\Phi|(E-H_{\text{eff}})\mathscr{A}(\Phi w_i^{(+)})\rangle \\ &= -\left\langle W_{0,f}^{(-)}\Phi|(E-H_{\text{eff}})\mathscr{A}\left\{\Phi\left(\frac{1}{1-\hat{K}'}\right)W_i^{(+)}\right\}\right\rangle \end{aligned} \tag{2.47}$$

and the alternative expression

$$\hat{\mathscr{T}}_{fi} = -\langle \mathscr{A}(\Phi W_f^{(-)}) | (E - H_{\text{eff}}) W_{0,i}^{(+)} \Phi \rangle$$
$$= -\left\langle \mathscr{A}\left(\frac{1}{1-\hat{K}'} W_f^{(-)} \right) \middle| (E - H_{\text{eff}}) W_{0,i}^{(+)} \Phi \right\rangle \tag{2.48}$$

The circumflex on $\hat{\mathscr{T}}$ is a reminder that $\hat{\mathscr{T}}$ is a matrix and that one must specify the initial and final states. For the stripping (d,p) reaction, $W_{0,f}^{(-)}\Phi$ in (2.47) is, according to (2.33), the proton–nucleus unperturbed final-state wave function $U_{0,f}^{(-)}\phi$. The function $W_i^{(+)}\Phi$ is the exact initial channel deuteron nucleus wave function $\chi\psi v_i^{(+)}$. With these substitutes, (2.47) and (2.33) become identical. One can then obtain (2.37) for $\mathscr{T}_{dp}$. This result is referred to as the *postrepresentation* of the transition amplitude, since it involves the residual interaction in the final channel, $\mathscr{V}^{(f)}$.

In using (2.48) to obtain an expression for the stripping transition amplitude, the unperturbed initial state is given by $\chi\psi V_{0,i}^{(+)}$; the final-state component of interest is $\phi u_f^{(-)}$. Thus one obtains

$$\mathscr{T}_{dp} = -\left\langle \mathscr{A}\left\{ \left(\phi \left(\frac{1}{1-\hat{K}'} \right)_{uu} + \chi\psi \left(\frac{1}{1-\hat{K}'} \right)_{vu} \right) U_f^{(-)} \right\} \middle| (E - H_{\text{eff}}) \chi\psi V_{0,i}^{(+)} \right\rangle \tag{2.49}$$

We now introduce the Hamiltonian H_i for the initial channel

$$H_i(\chi\psi V_{0,i}^{(+)}) = E(\chi\psi V_{0,i}^{(+)}) \tag{2.50}$$

and the residual potential in the initial channel, $\mathscr{V}^{(i)}$:

$$\mathscr{V}^{(i)} \equiv H_{\text{eff}} - H_i \tag{2.51}$$

Equation (2.49) then becomes

$$\mathscr{T}_{dp} = \left\langle \mathscr{A}\left\{ \left(\phi \left(\frac{1}{1-\hat{K}'} \right)_{uu} + \chi\psi \left(\frac{1}{1-\hat{K}'} \right)_{vu} \right) U_f^{(-)} \right\} \middle| \mathscr{V}^{(i)} (\chi\psi V_{0,i}^{(+)}) \right\rangle \tag{2.52}$$

which should be compared with (2.37). This is known as the *priori* representation, since it involves the residual interaction in the initial channel. The analog of the (2.46′) becomes, upon neglecting K_{uv},

$$\mathscr{T}_{dp}^{(\text{DWA})} = \langle \mathscr{A} u_{0,f}^{(-)} \phi | \mathscr{V}^{(i)} v_{0,i}^{(+)} \chi\psi \rangle \tag{2.53}$$

The two expressions (2.52) and (2.33) are equal numerically if no further approximations are made. Which one is used is a matter of convenience, as approximations in their evaluation may be made with greater validity when

one rather than the other is used, as we shall see. We emphasizé once more that the use of the operator $\hat{K}'$ is essential if antisymmetry, overlap, and continuum effects are to be properly included.

3. APPLICATIONS

This section is concerned with the implementation of the discussion of the preceding section to the process of stripping. The starting point is the post-transition (or the corresponding prior transition) matrix element given by (2.37) and the DWA form (2.46), in which overlap and the perturbation of the deuteron–target nucleus wave function arising from the possibility of the transition to the proton–nucleus system are neglected. (The error resulting from this last approximation is reduced considerably by the use of a semiempirical potential between the deuteron and the target nucleus, which to some extent must include the effects of the two-step processes, in which, for example, the neutron is stripped from the deuteron by the target nucleus and then in the second step is picked up by the proton to reform the deuteron.) Elements entering into the calculation consist of the initial and final wave functions and the residual interactions $\mathscr{V}^{(f)}$ or $\mathscr{V}^{(i)}$.

According to (2.36),

$$\mathscr{V}^{(f)} = H_{\text{eff}} - H_f$$

The Hamiltonian H_{eff} is generally chosen to be of the form

$$H_{\text{eff}} = H_A + T_0 + T_1 + w_{0,A} + w_{1,A} + w(0,1) \tag{3.1}$$

where H_A is the Hamiltonian for the target nucleus, T_1 and T_0 the kinetic energy operators for the neutron and proton, $w_{0,A}$ is the interaction of the proton with the target nucleus, $w_{1,A}$ that of the neutron, and $w(0,1)$ the neutron–proton interaction. The final Hamiltonian is given by

$$H_f = H_A + T_1 + w_{1,A} + T_0 + w \tag{3.2a}$$

$$= H_{A+1} + T_0 + w \tag{3.2b}$$

Here w is a mean, generally complex potential representing the interaction between the proton and the residual $(A+1)$ nucleus. Taking the difference between (3.2) and (3.1) yields

$$\begin{aligned}\mathscr{V}^{(f)} &= w_{0,A} + w(0,1) - w \\ &= \sum_{i=1}^{A+1} w(0,i) - w\end{aligned} \tag{3.3}$$

The mean potential w cannot induce any transitions, so that its (d, p) matrix element vanishes. Hence, from (2.46′),

$$\mathcal{T}_{dp}^{(\mathrm{DWA})} = \left\langle U_{0,f}^{(-)}\phi \middle| \sum_{i=1}^{A+1} w(0,i)\mathcal{A}(v_{0,i}^{(+)}\chi\psi) \right\rangle \tag{3.4}$$

One now makes the *spectator* approximation. Qualitatively it is assumed that the proton does not participate in the reaction. More precisely, one assumes that the only terms in the sum over $w(0,i)$ that contribute significantly to $\mathcal{T}_{dp}$ are those for which the nucleons denoted by i are neutrons. Moreover, since the wave function ϕ, as well as the indicated initial state, are antisymmetric in the neutron coordinates, one obtains

$$\mathcal{T}_{dp}^{(\mathrm{DWA})} \simeq (N_A + 1)\langle U_{0,f}^{(-)}\phi | w(0,1)\mathcal{A}(v_{0,i}^{(+)}\chi\psi)\rangle \tag{3.5}$$

where N_A is the number of neutrons in the target nucleus. Finally, if the exchange integrals in this equation are small, as is often the case, one obtains the simple result

$$\mathcal{T}_{dp}^{(\mathrm{DWA})} \simeq (N_A + 1)\langle U_{0,f}^{(-)}\phi | w(0,1)v_{0,i}^{(+)}\chi\psi\rangle \tag{3.6}$$

Forms (3.5) and (3.6) are most convenient because $w(0,1)$ has a short range, so that domains in which the neutron–proton separation is large do not contribute to $\mathcal{T}_{dp}$. Exploiting this feature leads to a considerable simplification, as we shall now show.

We need to make explicit the spatial arguments of the functions occurring in (3.5). The function χ as well as $w(0,1)$ depends on $\mathbf{r}_1 - \mathbf{r}_0$, where $\mathbf{r}_0$ is the proton coordinate and $\mathbf{r}_1$ the neutron. The function v depends on the separation of the deuteron center of mass from the center of mass, $\mathbf{r}_A$, of the target nucleus: that is,

$$\mathbf{r}_D \equiv \mathbf{r}_A - \tfrac{1}{2}(\mathbf{r}_1 + \mathbf{r}_0) = \mathbf{r}_A - \mathbf{r}_1 + \frac{\mathbf{r}_1 - \mathbf{r}_0}{2} \tag{3.7}$$

The function U depends on the separation of the proton from the center of mass of the target nucleus and the neutron:

$$\mathbf{r}_p = \frac{A\mathbf{r}_A + \mathbf{r}_1}{A+1} - \mathbf{r}_0 = \frac{A}{A+1}(\mathbf{r}_A - \mathbf{r}_1) + \mathbf{r}_1 - \mathbf{r}_0 \tag{3.8}$$

Equation (3.6) becomes

$$\mathcal{T}_{dp}^{(\mathrm{DWA})} = \int d\mathbf{r}_p \int d\mathbf{r}_D \int d\mathbf{r}_2 \cdots U_{0,f}^{(-)*}(\mathbf{r}_p)\phi_f^*(\mathbf{r}_1 - \mathbf{r}_A, \mathbf{r}_2 - \mathbf{r}_A, \ldots)$$
$$\times w(\mathbf{r}_1 - \mathbf{r}_0)v_{0,i}^{(+)}(\mathbf{r}_D)\chi(\mathbf{r}_1 - \mathbf{r}_0)\psi_i(\mathbf{r}_2 - \mathbf{r}_A, \mathbf{r}_3 - \mathbf{r}_A, \ldots)$$

Performing the integration over $\mathbf{r}_2, \mathbf{r}_3, \cdots$ yields

$$\langle \phi_f(\mathbf{r}_1 - \mathbf{r}_A, \mathbf{r}_2 - \mathbf{r}_A, \cdots) | \psi_i(\mathbf{r}_2 - \mathbf{r}_A, \mathbf{r}_3 - \mathbf{r}_A, \cdots) \rangle = f^*_{fi}(\mathbf{r}_1 - \mathbf{r}_A) \tag{3.9}$$

so that

$$\mathcal{T}^{(\mathrm{DWA})}_{dp} = (N_A + 1) \int d\mathbf{r}_p \int d\mathbf{r}_D U^{(-)*}_{0,f}(\mathbf{r}_p) f^*_{fi}(\mathbf{r}_1 - \mathbf{r}_A) w(\mathbf{r}_1 - \mathbf{r}_0) \chi(\mathbf{r}_1 - \mathbf{r}_0) v^{(+)}_{0,i}(\mathbf{r}_D) \tag{3.10}$$

We now evaluate $w\chi$ in the limit of zero range of the neutron–proton potential. Neglecting the tensor force between neutron and proton, the Schrödinger equation satisfied by χ is

$$\nabla^2 \chi + \left(-\gamma^2 - \frac{m}{\hbar^2} w \right) \chi = 0 \tag{3.11}$$

where the dependent variable is $\mathbf{r}_1 - \mathbf{r}_0$. The eigenvalue γ^2 is related to the binding energy B of the deuteron by

$$\gamma^2 = \frac{\hbar^2}{m} B$$

Solving (3.11) for $w\chi$ yields

$$w\chi = \frac{\hbar^2}{m} (\nabla^2 - \gamma^2) \chi \tag{3.12}$$

For zero range w,

$$\chi = N e^{-\gamma r}/r \equiv N \frac{u}{r} \tag{3.13}$$

where N is the normalization. N can be expressed in terms of the effective range ρ_t,

$$\rho_t \equiv 2 \int_0^\infty (e^{-2\gamma r} - u^2)\, dr$$

It follows that

$$\int_0^\infty u^2\, dr = \frac{1 - \gamma \rho_t}{2\gamma}$$

But

$$\int_0^\infty \chi^2 \, d\mathbf{r} = 1 = 4\pi N^2 \int_0^\infty u^2 \, dr = 4\pi N^2 \frac{1 - \gamma\rho_t}{2\gamma}$$

Solving for N yields

$$N = \frac{1}{\sqrt{4\pi}} \left(\frac{2\gamma}{1 - \gamma\rho_t} \right)^{1/2} \tag{3.14}$$

The current value of ρ_t is 1.767 fm.

Inserting (3.13) into (3.12) yields

$$w\chi = \sqrt{4\pi} \left(\frac{2\gamma}{1 - \gamma\rho_t} \right)^{1/2} \frac{\hbar^2}{m} \delta(\mathbf{r}) \tag{3.15}$$

We can now return to (3.10) and replace the integration variables $\mathbf{r}_p$ and $\mathbf{r}_0$ by $\mathbf{r}_A - \mathbf{r}_1 \equiv \mathbf{R}$ and $\mathbf{r} \equiv \mathbf{r}_1 - \mathbf{r}_0$. Integrating over $\mathbf{r}$, one obtains, including the Jacobian of the transformation,

$$\mathcal{T}_{dp}^{(\mathrm{DWA})} = \sqrt{4\pi} \frac{\hbar^2}{m} \left(\frac{2\gamma}{1 - \gamma\rho_t} \right)^{1/2} \frac{A+2}{2(A+1)} (N_A + 1)$$
$$\times \int d\mathbf{R} U_{0,f}^{(-)*} \left(\frac{A}{A+1} \mathbf{R} \right) f_{fi}^*(-\mathbf{R}) v_{0,i}^{(+)}(\mathbf{R}) \tag{3.16}$$

The zero range approximation reduced the six-dimensional integral, (3.10), to a three-dimensional one. The latter is readily evaluated by expanding $U^{(-)}$ and $v^{(+)}$ in a partial wave series, so that (3.16) becomes, after making the relatively simple angular integration and evaluating spin matrix elements, a sum of one-dimensional integrals. The function $U_{0,f}^{(-)}$ is generally taken from the optical model analyses of the proton–nucleus interaction described in Chapter V. A similar optical model analysis has been made of the deuteron–nucleus interaction. However, it should be remembered that an understanding of the latter is based on a much smaller data pool than that available from the proton–nucleus interaction. A table of optical model parameters for the deuteron projectile is given in Section 4.

The overlap function $f_{fi}(\mathbf{R})$ is, in the independent-particle description of the nucleus, proportional to a single-particle wave function. As we discussed earlier, the residual interactions will add multiparticle components to the nuclear wavefunctions. However, these cannot contribute to f_{fi} and to $\mathcal{T}_{dp}^{(\mathrm{DWA})}$. Thus the effect of the residual interaction is to reduce the strength of the single-particle component since the total nuclear wave function is normalized to unity. This

is taken into account by the introduction of the *spectroscopic factor* $\mathscr{S}$ [see (1.5)]:

$$f_{fi}(R) = \frac{\mathscr{S}^{1/2}(\alpha, j)\phi_j(\mathbf{R})}{\sqrt{N_A + 1}} \tag{3.17}$$

Putting the arguments of $\mathscr{S}^{1/2}$ equal only to the angular momentum j of the neutron single-particle orbital ϕ_j is an assumption, since in principle f_{fi} could depend on other properties of the initial and final nuclei. The function ϕ_j is assumed to be orthogonal to ψ. We remind the reader that in the limit of the independent-particle model, when the target is a closed-shell nucleus, $\mathscr{S}$, with the normalization above, is unity. This completes the description of the various factors entering into (3.16) for the transition matrix $\mathscr{T}_{dp}$.

Some qualitative conclusions that follow from (3.16) for the transition matrix $\mathscr{T}_{dp}^{(\mathrm{DWA})}$ can now be drawn. Since both the $U^{(-)}$ and $v^{(+)}$ are wave functions describing the motion of particles in an absorptive potential, their magnitudes will be reduced in the nuclear interior. As a consequence, those partial waves of $U^{(-)}$ and $v^{(+)}$ that are large at the nuclear surface will make the most important contribution to the transition matrix. Roughly, this will occur for those partial waves l_i and l_f of $v^{(+)}$ and $U^{(-)}$, respectively, satisfying the conditions

$$k_D R \sim l_i \tag{3.18}$$

$$\frac{Ak_p}{A+1} R \sim l_f \tag{3.19}$$

Hence the orbital angular momentum L of the single-particle nuclear wave function ϕ of (3.17) which will be most strongly populated will satisfy the condition

$$\mathbf{L} = \mathbf{l}_i - \mathbf{l}_f \tag{3.20}$$

Under these circumstances (large absorption) the (d,p) reaction is a surface reaction,

These conclusions can easily be deduced from the overlap integral in (3.16) by making a partial wave series for $U^{(-)}$ and $u^{(+)}$. For this purpose it is not necessary to take spin onto account, so that

$$v_{0,i}^{(+)} = \sum_{l_i} (2l_i + 1) i^{l_i} P_{l_i}(\hat{\mathbf{k}}_i \cdot \hat{\mathbf{r}}) e^{i\delta_{l_i}} \phi_{l_i}(r) = \sqrt{4\pi} \sum \sqrt{2l_i + 1}\, i^{l_i} Y_{l_i,0} e^{i\delta_{l_i}} \varphi_{l_i}(r) \tag{3.21}$$

and

$$\begin{aligned} U_{0,f}^{(-)*} &= \sum_{l_f} (2l_f + 1) i^{-l_f} P_{l_f}(\hat{\mathbf{k}}_f \cdot \hat{\mathbf{r}}) e^{i\delta_{l_f}} \psi_{l_f}(r) \\ &= 4\pi \sum_{l_f, m_f} i^{-l_f} e^{i\delta_{l_f}} Y_{l_f m_f}(\hat{\mathbf{k}}_i \cdot \hat{\mathbf{k}}_f) Y_{l_f, m_f}^{*}(\hat{\mathbf{k}}_i \cdot \hat{\mathbf{r}}) \psi_{l_f}(r) \end{aligned} \tag{3.22}$$

Finally, let

$$\phi_j(\mathbf{r}) = \chi_L(r)\, Y_{LM}(\hat{\mathbf{k}}_i \cdot \hat{\mathbf{r}})$$

The transition matrix becomes

$$\mathcal{T}_{dp}^{(\mathrm{DWA})} = (4\pi)^2 \frac{\hbar^2}{m}\left(\frac{2\gamma}{1-\gamma\rho_t}\right)^{1/2} \mathcal{S}^{1/2}(\alpha, L)\sqrt{N_A + 1}\,\frac{A+2}{2(A+1)}$$
$$\times \sum_{l_i, l_f} \sqrt{2l_i+1}\, i^{l_i - l_f} e^{i(\delta_{l_i} + \delta_{l_f})} I(l_i, l_f, L)\, Y_{l_f, m_f}(\hat{\mathbf{k}}_i \cdot \hat{\mathbf{k}}_f)$$
$$\times \int d\Omega\, Y_{l_i,0}\, Y^*_{l_f,m_f}\, Y^*_{LM}$$

where

$$I(l_i, l_f, L) = \int \psi_{L_f} \varphi_{l_i} \chi_L r^2\, dr \tag{3.23}$$

The angular integral can be performed using (A.2.35) from the Appendix in deShalit and Feshbach (74):

$$\int d\Omega\, Y_{l_i,0}\, Y^*_{l_f,m_f}\, Y^*_{LM} = \left[\frac{(2l_i+1)(2l_f+1)(2L+1)}{4\pi}\right]^{1/2}$$
$$\times \begin{pmatrix} l_i & L & l_f \\ 0 & M & m_f \end{pmatrix}\begin{pmatrix} l_i & L & l_f \\ 0 & 0 & 0 \end{pmatrix}$$

so that

$$\mathcal{T}_{dp}^{(\mathrm{DWA})} = (4\pi)^{3/2} \frac{\hbar^2}{m}\left(\frac{2\gamma}{1-\gamma\rho_t}\right)^{1/2} \mathcal{S}^{1/2}(\alpha, L)\sqrt{N_A + 1}\,\frac{A+2}{2(A+1)}$$
$$\times \sum_{l_i, l_f} \sqrt{2l_i+1}\, i^{l_i - l_f} e^{i(\delta_{l_i} + \delta_{l_f})} I(l_i, l_f, L)\, Y_{l_f, m_f}(\hat{\mathbf{k}}_i \cdot \hat{\mathbf{k}}_f)$$
$$\times [(2l_i+1)(2l_f+1)(2L+1)]^{1/2}\begin{pmatrix} l_i & L & l_f \\ 0 & M & m_f \end{pmatrix}\begin{pmatrix} l_i & L & l_f \\ 0 & 0 & 0 \end{pmatrix} \tag{3.24}$$

The $3-j$ coefficients yield not only the angular momentum conservation condition of (3.20) but parity conservation as well, since $l_i + L + l_f$ must be even. The magnitude of the factor $\exp[i(\delta_{l_i} + \delta_{l_f})]$, is, for absorption optical potentials, much less than unity for small l's rising sharply to unity at the grazing values of l_i and l_f given approximately by (3.18) and (3.19). The integral I will tend to zero as l_i and l_f exceed these grazing values since the corresponding angular

momentum barriers become important beyond the nuclear radius. The integral I will be small for these values of l_i and l_f for which the absorption is large, that is, for l_i and l_f considerably smaller than the grazing values. As Austern (61) pointed out, this is a consequence of destructive interference between the optical model deuteron and proton wave functions. As the reader should verify, the radial wave functions for each of these waves inside the nuclear interior will for the most part be of the form $\exp(-iKr)/r$, where K is the internal

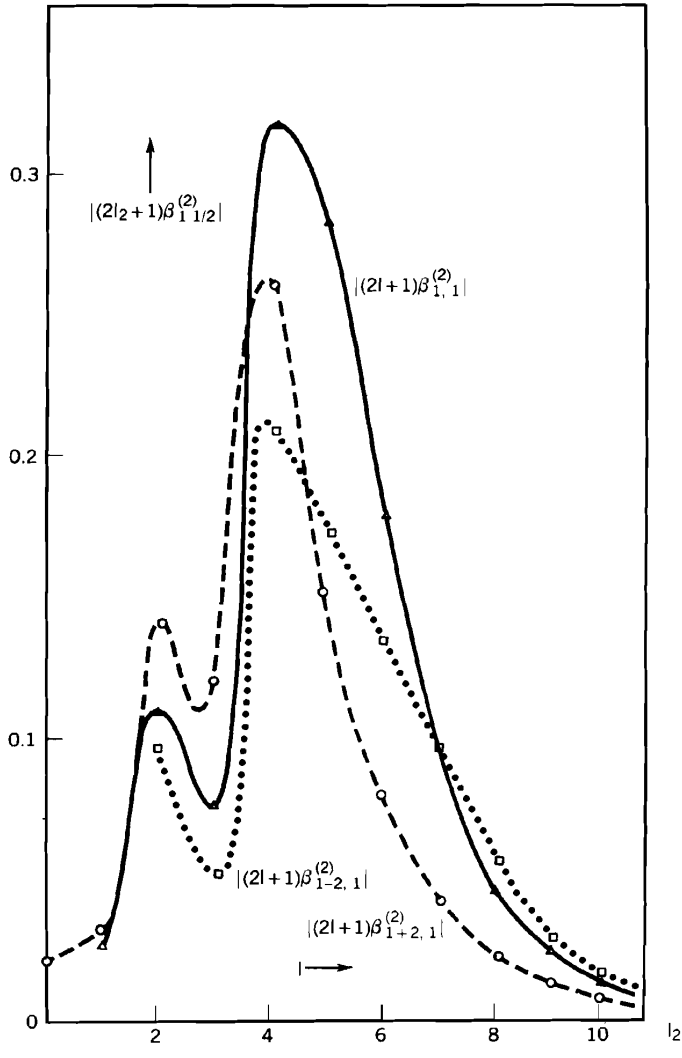

FIG. 3.1. The l window. The modulus of the stripping integrals contributing to an $\Delta l = 2$ transfer reaction ^{24}Mg (d, p) ^{25}Mg, ground state at $E_d = 10.1$ MeV plotted against $l_2 = l_f$. [From Hooper (66).]

momentum appropriate for each particle. This is not correct near $r = 0$, but in that region the magnitude of the deuteron wave function is small as a consequence of the absorption. Elsewhere the product in the integral of I will fluctuate strongly and I will be small.

These arguments demonstrate the existence of an l window—that there is a range in l_f and l_i, respectively, for which $\exp(\delta_{l_i} + \delta_{l_f})I$ is appreciable. It is negligible if l_i or l_f fall outside these ranges. This is illustrated in Fig. 3.1.

The impact of the l *window* on the angular distribution can be seen from (3.24). The angular distribution will be oscillatory with a frequency that will lie between $\pi/2l_{\max}$ and $\pi/2l_{\min}$, where $l_{\max}$ and $l_{\min}$ are the maximum and minimum values of l_f or l_i.

Examination of the integral I yields another qualitative result that could have been anticipated—that the momentum transfer is bounded by the "momentum" of the captured neutron. That is,

$$\left|\frac{A}{A+1}k_f - k_i\right| < \sqrt{\frac{2m}{\hbar^2}|\varepsilon|} \tag{3.25}$$

where $|\varepsilon|$, the binding energy of the captured neutron, is given by the Q of the reaction plus the binding energy of the deuteron, 2.246 MeV. As k_f and k_i increase, this inequality implies that the reaction proceeds when k_f is about equal to k_i, this is, for good *momentum matching*. "Good momentum matching gives slow radial oscillations and large overlaps only in the nuclear surface region where the distorted wave functions are not yet affected by absorption" [Austern, Iseri et al (87)]. Since when multiplied by the nuclear radius, the left-hand side of this inequality gives the maximum angular momentum transfer L, we see that for a given (d, p) reaction, L is generally limited to fairly small values.

The discussion above does not take the spin variable into account. For a given L of the captured neutron, two values of j, its total angular momentum, $L \pm \frac{1}{2}$, are possible. These correspond to two different single-particle states and therefore to two different radial wave functions χ_L, so that I is spin dependent. The spin dependence of the proton and deuteron optical potential as well as the deuteron D state will give $\mathscr{T}$ additional spin dependence. However, the net effect is quite small, although it may be observable, as indicated by Fig. 3.2. A deep minimum at the back angles is seen for the $l = 1$ transfer for $p_{1/2}$ and not for $p_{3/2}$. The spin dependence is much more dramatically revealed in experiments that measure the polarization of the proton, or if the deuteron beam is polarized, the vector analyzing power, as illustrated in Fig. 3.3. (Polarization is discussed in Appendix C.)

When spin is included in the discussion, the angular momentum balance must be reconsidered. If $\mathbf{J}_i$ is the spin of the target nucleus, $\mathbf{s}_D$ that of the deuteron, $\mathbf{J}_f$ that of the final nucleus, and $\mathbf{s}_p$ the spin of the proton, conservation of angular momentum requires that

$$\mathbf{J}_i + \mathbf{s}_D + \mathbf{l}_i = \mathbf{J}_f + \mathbf{s}_p + \mathbf{l}_f \tag{3.26}$$

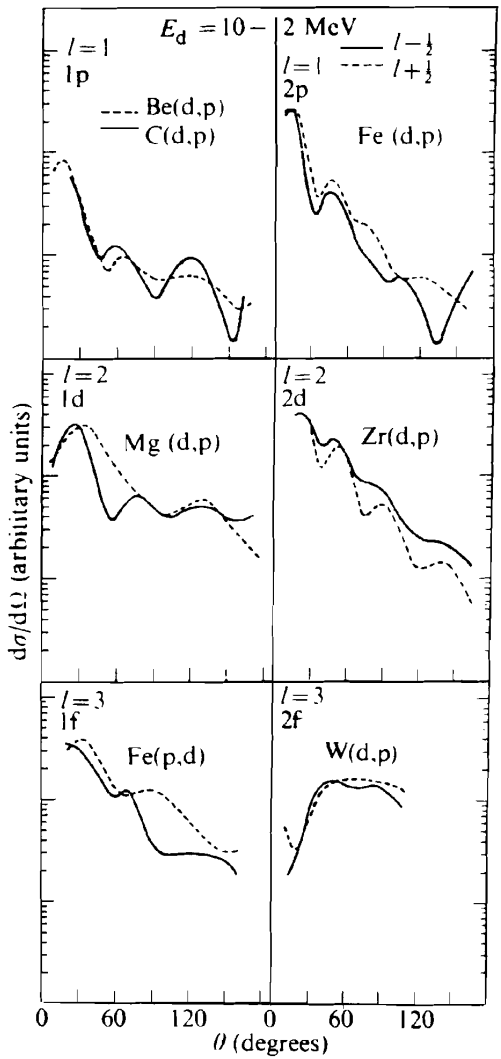

FIG. 3.2. Summary of j-dependent effects in (d, p) reactions. The curves represent the trend of the experimental data for different j values [Schiffer (68)]. [From Barrett and Jackson (77).]

The assumption that the transferred neutron is in a single-particle state leads to the requirement

$$\mathbf{J}_f = \mathbf{J}_i + \mathbf{j}_n = \mathbf{J}_i + \mathbf{L} + \mathbf{s}_n \tag{3.27}$$

where $\mathbf{L}$ and $\mathbf{s}_n$ are the angular momentum and spin of the neutron. Substituting (3.27) into (3.26) yields

$$\mathbf{s}_d + \mathbf{l}_i = \mathbf{L} + \mathbf{l}_f + \mathbf{s}_n + \mathbf{s}_p$$

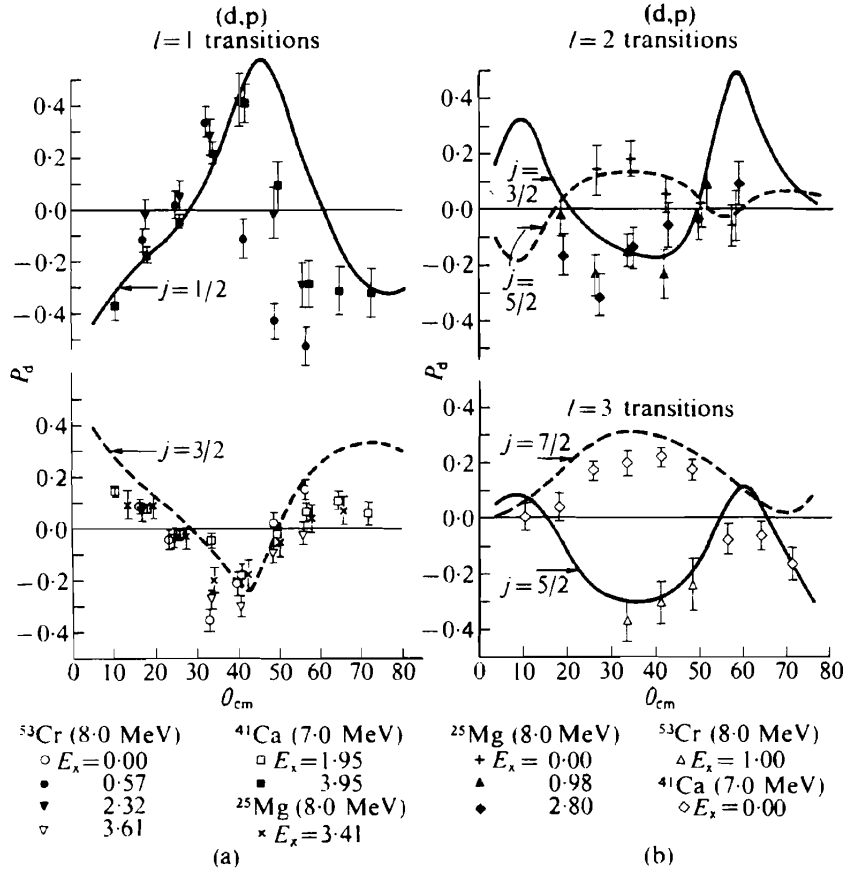

FIG. 3.3. Vector analyzing power for various (d,p) reactions [Glashauser and Thirion (69)]. [From Barrett and Jackson (77).]

Presuming the absence of spin-dependent terms in the optical potentials of the proton and deuteron and in the neutron–proton potential yields (3.20). Hence the equation above reduces to the obvious result

$$\mathbf{s}_d = \mathbf{s}_n + \mathbf{s}_p$$

Since the deuteron is in a spin-1 state, the captured neutron and the emerging proton must also be in a spin-1 state. If the deuteron spin is parallel or antiparallel to the normal to the scattering plane, the bound neutron and the emergent proton spins will be parallel. If the spin of the deuteron lies in the plane, the neutron and proton spins will be antiparallel. If the incident deuteron beam is unpolarized, the three deuteron spin states will have equal populations.

Therefore, the neutron and the proton spin will be parallel on the average. Hence by observing the emerging proton spin, one determines the captured neutron spin and therefore the total angular momentum, $L \pm \frac{1}{2}$, of the neutron state. We shall leave the verification of the discussion above as an exercise for the reader.

The cross section is obtained by squaring $\mathscr{T}$, given by (3.24), summing over m_f, averaging over the deuteron spin, and multiplying by the ratio of the emitted current to the incident current. The latter contains the factor $(N_A + 1)$. One obtains

$$\frac{d\sigma_{d,p}}{d\Omega} = \frac{1}{3}\left(\frac{A+2}{A+1}\right)^2 \frac{k_f}{k_i}\frac{\mu_i\mu_f}{m^2}\left(\frac{2\gamma}{1-\gamma\rho_t}\right)\mathscr{S}(\alpha, L)(2L+1)\sum_{\substack{l_i l_i' \\ l_f l_f' \\ l}}(-)^l(2l+1)(2l_i+1)(2l_i'+1)$$

$$\times(2l_f+1)(2l_f'+1)e^{i(\delta_{l_i}+\delta_{l_f}-\delta_{l_i'}^*-\delta_{l_f'}^*)}\begin{pmatrix} l_i & L & l_f \\ 0 & 0 & 0\end{pmatrix}\begin{pmatrix} l_i' & L & l_f' \\ 0 & 0 & 0\end{pmatrix}$$

$$\times\begin{pmatrix} l_f & l_f' & l \\ 0 & 0 & 0\end{pmatrix}\begin{pmatrix} l_i & l_i' & l \\ 0 & 0 & 0\end{pmatrix}\begin{Bmatrix} l_i & l_i' & l \\ l_f' & l_f & L\end{Bmatrix} I(l_i l_f L) I^*(l_i' l_f' L) P_l(\cos\vartheta) \qquad (3.28)$$

This formula is less formidable than it looks because the sums on $l_i l_i'$, l_f, and l_f' are over a limited range because of the l window discussed earlier.‡ The sum over l is limited as a consequence. We also see that the maximum value of l is the least of the maximum values of $2l_i$ and $2l_f$.

The derivation of (3.28) makes a number of approximation that we shall now review. We have mentioned the neglect of spin-dependent terms in the proton and deuteron optical potentials as well as the D component of the deuteron wave function. Because these terms are comparatively small, a perturbation treatment is useful [see Satchler (83, p. 384)]. The inclusion of spin-orbit coupling in the optical potentials will not modify the angular distributions greatly. However, the overall magnitude and therefore the spectroscopic factors extracted from the data can be changed substantially [Lee, Schiffer, et al. (64); Seth, Biggerstaff, Miller, and Satchler (67)]. There are special effects. For example, as we noted above, a systematic effect for $l = 1$ transfer is observable. The spin-orbit coupling in the optical potentials is responsible [Lee, Schiffer, et al. (64)]. A similar effect is seen for $l = 2$ and $l = 3$ transfers. In this case both the spin-orbit coupling in the optical potentials and the D state of the deuteron are sources of the effect [Delic and Robson (74)].

We turn next to the zero range approximation, (3.13) and (3.15). To obtain

‡Highly developed computer codes make comparison of experiment with stripping theory correspondingly straightforward.

the next order, return to (3.10) and insert the variables given by (3.7) and (3.8):

$$\mathcal{T}_{dp}^{(\mathrm{DWA})} = \frac{A+2}{2(A+1)}(N_A+1)\int d\mathbf{r}\int d\mathbf{R}\, U_{0,f}^{(-)*}\left(\frac{A}{A+1}\mathbf{R}+\mathbf{r}\right) \times f_{fi}^{*}(-\mathbf{R})w(\mathbf{r})\chi(\mathbf{r})v_{0,i}^{(+)}(\mathbf{R}+\tfrac{1}{2}\mathbf{r}) \tag{3.29}$$

The next step is to expand $U_{0,f}^{(-)}$ and $v_{0,i}^{(+)}$ in a Taylor series in $\mathbf{r}$ and perform the $\mathbf{r}$ integration assuming that $w(\mathbf{r})\chi(\mathbf{r})$ is spherically symmetrical. One then obtains after some simple manipulations

$$\mathcal{T}_{dp}^{(\mathrm{DWA})} = \frac{A+2}{2(A+1)}(N_A+1)B\int d\mathbf{R}\, U_{0,f}^{(-)}\left(\frac{A}{A+1}\mathbf{R}\right)f_{fi}^{*}(-\mathbf{R})v_{0,i}^{(+)}(\mathbf{R}) \times\left\{1+\tfrac{1}{6}\rho\left(\frac{m}{\hbar^2}\right)\left[\mathcal{V}_n(\mathbf{R})+\mathcal{V}_p\left(\frac{A}{A+1}\mathbf{R}\right)-\mathcal{V}_D(\mathbf{R})+B\right]\right\} \tag{3.30}$$

where

$$B \equiv \int d\mathbf{r}\, w\chi \tag{3.31a}$$

$$\rho B = \int d\mathbf{r}\, r^2 w\chi \tag{3.31b}$$

The potentials $\mathcal{V}_n$, $\mathcal{V}_p$, and $\mathcal{V}_D$ are, respectively, the binding potential of the neutron, the optical potential for the proton, and the optical potential for the deuteron. B is given by $(E_D + |E_n| - E_p)$, where $|E_n|$ is the binding energy of the neutron. In deriving (3.30) the limit of $A \to \infty$ was taken except for the argument of $\mathcal{V}_p$.

As one can immediately verify, when (3.15) is used, the first term, independent of ρ, of (3.30) agrees with (3.16). The use of (3.31*a*) provides some flexibility, however, since it makes possible the use of a more realistic expression for $w\chi$. The term proportional to ρ can readily be included in the calculations. The effect of the ρ term is to reduce the contributions from the interaction region. A comparison with the exact calculation is shown in Fig. 3.4. See Dickens, Drisco, Perey, and Satchler (65), Stock, Bock, et al. (67), and Santos (73) for further discussion.

In passing, note that the Perey effect (effective mass) will also reduce the amplitude of the proton and deuteron wave functions in the interaction region. The Perey effect is a consequence of the nonlocality and energy dependence of the optical potential.

Part of that nonlocality is generated by the Pauli principle, which tends to reduce the amplitude of the proton and neutron wave functions when they overlap the target and the residual nuclei. Antisymmetry can be included to

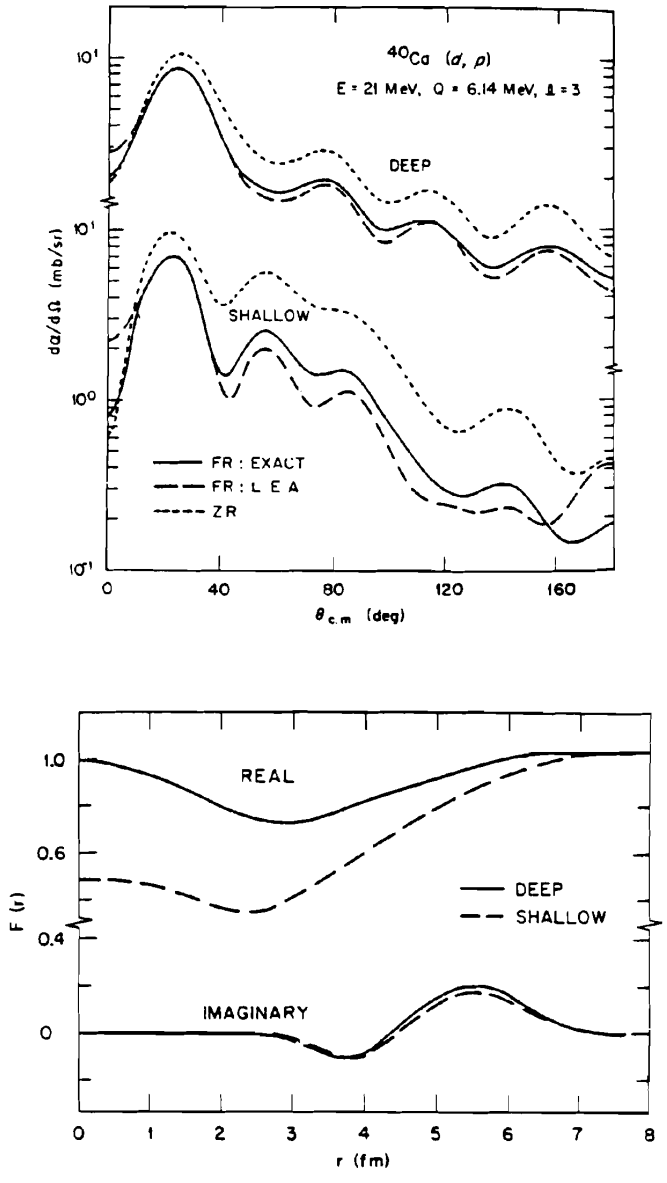

FIG. 3.4. Finite range effects. The dashed line is obtained using (3.30). $F(r)$ equals the expression within the braces in (3.30). The dotted line results from the use of the zero range approximation. The labels "shallow" and "deep" refer to the depth of the deuteron optical potential used ($V = 67$ MeV and 112 MeV, respectively). [From Satchler (83).]

some extent by adding in the exchange integral to (3.10). More accurately, the analysis of Section 2 should be used, including both the antisymmetry and nonorthogonality effects. That this is possible is demonstrated by the calculations of Döhnert (71) and those of several Japanese physicists, for example, Horiuchi (77). For an approximate treatment of antisymmetry that permits continued use of (3.1), see Johnson, Austern, and Hopes (82). The substantial agreement between DWA theory and experiment, particularly in the critical forward angle region, indicates that these effects, at least as far as the angular distribution is concerned, are small.

4. THE DEUTERON–NUCLEUS INTERACTION

The DWA amplitude depends strongly on the distorted deuteron wave function and therefore on the deuteron optical model. The deuteron has a comparatively large structure (diameter ~ 4.4 fm) and is very loosely bound (B.E. = 2.246 MeV). It can therefore readily "break up" when subjected to external forces provided by the target nucleus, a process that is aided by the Pauli exclusion principle. Deformation of the deuteron without breakup can also occur, but breakup is more likely. As a consequence, one finds strong deuteron absorption when the deuteron penetrates the nuclear interior. It is this strong absorption that is the most important factor in producing the l window of Section 3.

As in the nucleon case, one approach to the deuteron optical model potential has been empirical; that is, the parameters of an optical potential of an assumed form are adjusted so as to fit the observed deuteron–nucleus elastic scattering. A second approach attempts to relate the deuteron optical model with the underlying nucleon–nucleon forces. At a simple level, the folding model is used. It suffers from the obvious omission of the breakup channels and thus leads to a serious underestimate of the absorption component. A more complete treatment based on the general analysis developed in Chapter III and used in Section 2 of this chapter has been carried out by Döhnert (71). Döhnert includes the effects of antisymmetry, which involves the possible exchange of one or both of the deuteron nucleons with those in the target nucleus. The effects of breakup (as well as multistep processes) on stripping are included as well. This is ensured by the orthogonality conditions (2.5) and (2.6). However, the Döhnert procedure does not permit a calculation of the breakup that occurs in a deuteron–nucleus collision. A correct description of the nonlocality induced by the Pauli principle as well as the contribution coming from the finite size of the deuteron is thus obtained. One can at this point insert the nucleon–nucleon potentials as well as the wave functions for the target nucleus to obtain the deuteron optical model potential, recognizing from the beginning that only the elastic amplitude can be described by such a potential. Such a calculation does not seem to have been carried out for the deuteron [see Döhnert (71)], although Horiuchi (77) has performed the equivalent calculation for α-particle nucleus interaction. A less ambitious program employs the form derived by Dohnert for the empirical

analyses of the elastic scattering of the deuteron by the target nucleus, thereby avoiding the difficulties associated with the microscopic approach.

However, most of the analyses reported in the literature use directly a simple empirical form for the deuteron optical potential, similar to that employed for the nucleon optical potential described in Chapter V. The hope, underlying this convenient approach, is that the potential so obtained will yield wave functions that mimic the exact ones faithfully and so include effects such as antisymmetry and nonlocality implicitly. This can be the case only if the assumed form for the potential is sufficiently flexible so as to be capable of including the effects arising from nonlocality, such as the Perey effect (see p. 346).

The local form commonly used is [see (V.2.38)]

$$V_{\text{opt}}^{(D)} = \mathscr{V}_c + \mathbf{S}\cdot\mathbf{L}\mathscr{V}_{s0} \tag{4.1}$$

where

$$\mathscr{V}_c = V_{\text{Coul}} - Vf(x_0) - i\left[WF(x_W) - 4W_D \frac{d}{dx_D} f(x_D) \right]$$

$$\mathscr{V}_{s0} = \left(\frac{\hbar}{m_\pi c}\right)^2 V_{s0} \frac{1}{r}\frac{d}{dr} f(x_{s0})$$

and

$$f(x) = \frac{1}{1+e^x} \qquad x = \frac{r - r_i A^{1/3}}{a_i}$$

V, W, W_D, V_{s0} are constants, while r_i and a_i may have differing values for x_C, x_W, x_d, and x_{s0}. V_{Coul} is identical with that used in (V.2.38). $\mathbf{S}$ is the spin operator for the deuteron, normalized so that $S^2 = 2$.

A thorough analysis has been made of the data available at the time to obtain a global optical model for deuteron energies ranging from 12 to 90 MeV by Daehnick, Childs, and Vrcelj (DCV) (80) and for nuclei with mass between ^{37}Al and ^{238}Th. Their results are given in Table 4.1. Note that the DCV form assumes that $x_w = x_D$. As in the nucleon case, the central potential depth V decreases with increasing E, while the diffusivity grows with E. The volume absorption W is less important than the surface absorption W_D at the lower energies but is of equal importance at the highest energy. The diffusivity of the absorption potential, a_W, exhibits a dependence on neutron shell closure. The spin-orbit coupling decreases with increasing energy. Daehnick et al. (80) have also considered a complex spin-orbit coupling and have included in their table values of the parameters for nonrelativistic dynamics.

Examples of the quality of the fits obtained are given in Figs 4.1 to 4.4. The fits on the whole are quite good, although there are some deviations of significant size, but these are not systematic. Note that the ordinate scale is logarithmic. The authors believe that in part these may be a consequence of structure effects

TABLE 4.1 Recommended Global Parameter Prescriptions That Fit a Wide Range of Deuteron Scattering Data[a]

$V = 88.5 - 0.26E + 0.88ZA^{-1/3}$	MeV
$r_0 = 1.17$	fm
$a_0 = 0.709 + 0.0017E$	fm
$W = (12.2 + 0.0626E) \times (1 - e^{\beta})$	MeV
$W_D = (12.2 + 0.026E)e^{\beta}$	MeV
$r_W = 1.325$	fm
$a_W = 0.53 + 0.07A^{1/3} - 0.04\,\Sigma_i e^{-\mu_i}$	fm
$r_c = 1.30$	fm
$V_{s0} = 7.33 - 0.029E$	MeV
$r_{s0} = 1.07$	fm
$a_{s0} = 0.66$	fm

[a]Potential name: 79 DCV *L* (nonrelativistic kinematics only). *A*, mass number; *Z*, proton number; $\beta = -(E/100)^2$; $\mu_i = [(M_i - N)/2]^2$, where M_i = magic numbers (8, 20, 28, 50, 82, 126); *N*, neutron number; *E*, deuteron laboratory energy (MeV).

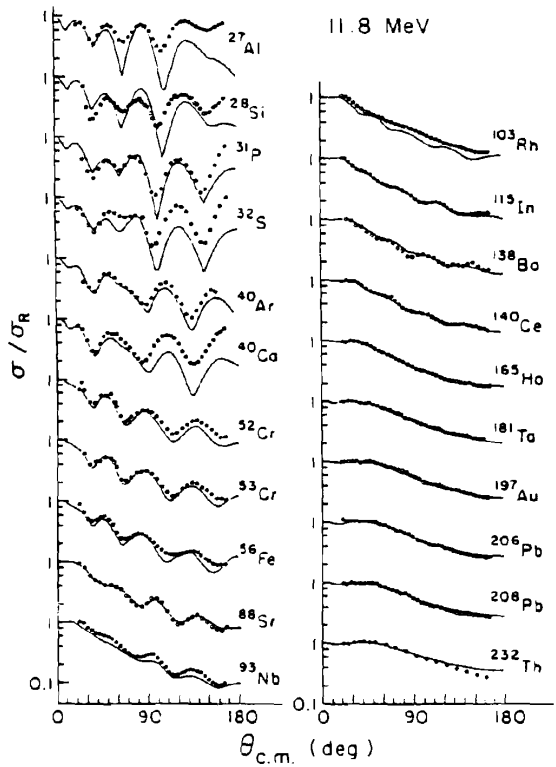

FIG. 4.1. Comparison of 11.8-MeV data with predictions of potential *L* (Table 4.1). [From Daehnick, Childs, and Vrcelj (80).]

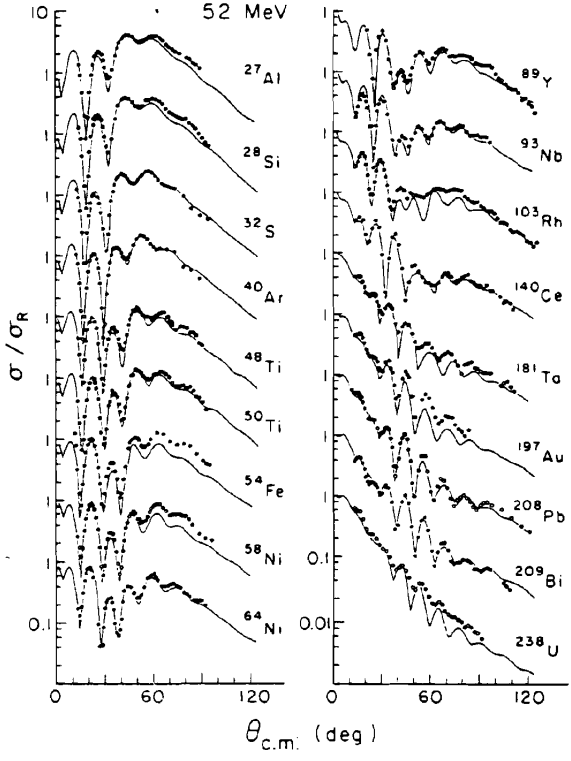

FIG. 4.2. Comparison of 52-MeV data with predictions of potential *L* (Table 4.1). [From Daehnick, Childs, and Vrcelj (80).]

and, at low energies, of contributions of compound elastic scattering. Resolution limitations are important for deformed nuclei targets when these have low-lying excited states. Reaction cross sections obtained from the optical model are systematically higher than the experimental values, indicating perhaps a need to modify the Woods–Saxon shape used in (4.1).

It is interesting to compare these phenomenological results with those obtained for the neutron–nucleus (*n*–nucleus) and proton–nucleus (*p*–nucleus interactions) (see Table V.2.1). We see that the real central (*d*–nucleus) potential is much greater than the corresponding nucleon potentials. Moreover, it differs substantially from the sum of the (*p*–nucleus) and *n*-nucleus real central interactions. However, the diffusivity a_0 is not very different. Both the imaginary central volume and surface terms, W and W_D, of the (*d*–nucleus) potential are very much larger than the corresponding nucleon–nucleus cases. The spin-orbit terms are not very different. Qualitatively, the difference in the real central deuteron potential from the sums of the nucleon potentials can be understood as a consequence of the finite size of the deuteron, while greater absorption

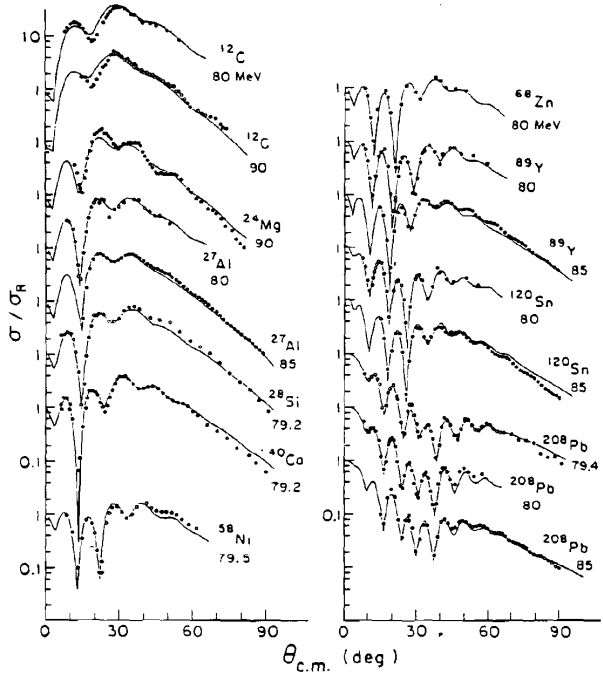

FIG. 4.3. Comparison of 80- to 90-MeV data with predictions of potential *L*, (Table 4.1). [From Daehnick, Childs, and Vrcelj (80).]

occurs because the penetrating deuteron breaks up readily in view of its small binding energy.

It has been pointed out that a two-step process involving breakup could be of some importance for stripping. The first step involves the breakup of the deuteron (i.e., a transition to the n–p continuum state) because of the interaction with the target nucleus followed by the capture of the neutron by the nucleus. In principle, this effect could be estimated using perturbation theory or the Dohnert procedure. Instead, the strategy in which the deuteron optical potential has been modified has been used. This has the convenience that the standard DWA formula whose evaluation by computer is a thoroughly tested and available procedure can be used. We discuss this approach in Section 6.

5. OVERLAP WAVE FUNCTION

The overlap wave function $f_{fi}(\mathbf{r})$ is defined as

$$f_{fi}(\mathbf{r}) = \langle \psi_i(\mathbf{r}_2, \mathbf{r}_3, \ldots) | \phi_f(\mathbf{r}, \mathbf{r}_2, \ldots) \rangle \tag{3.9}$$

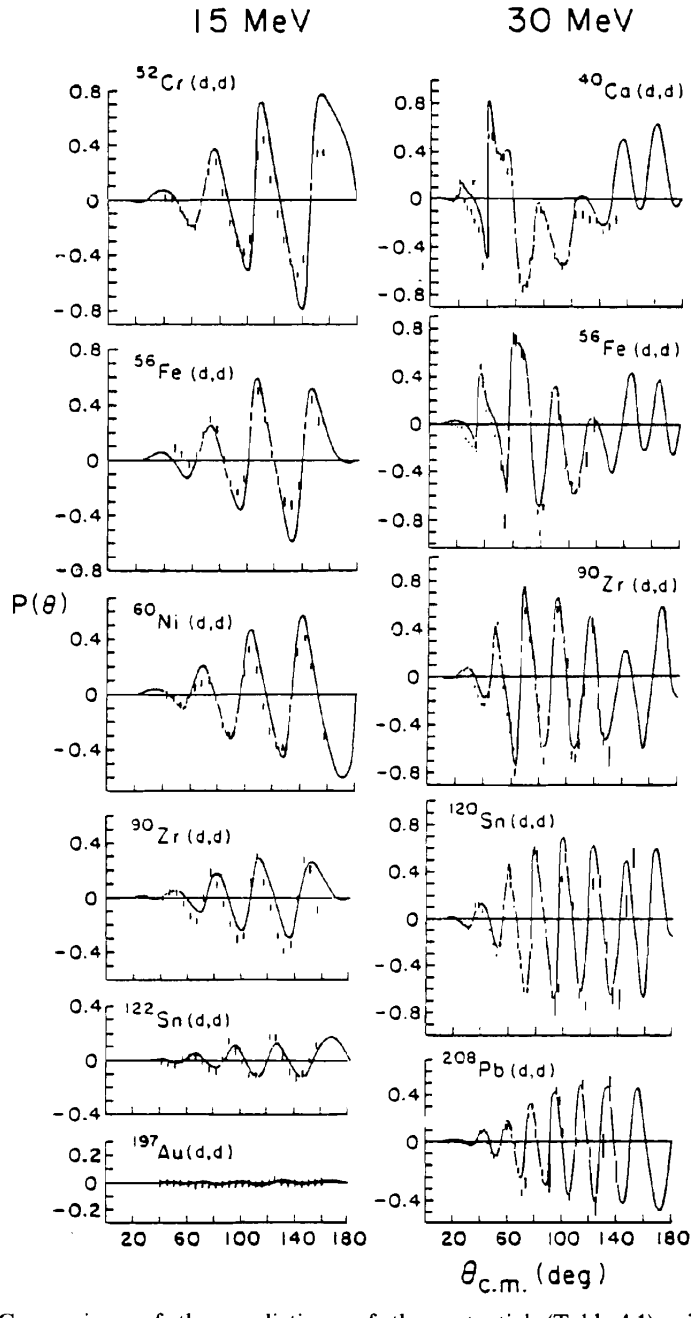

FIG. 4.4. Comparison of the predictions of the potential (Table 4.1) with vector polarization data. [From Daehnick, Childs, and Vrcelj (80).]

where integration over the coordinates common to ψ and ϕ_f is assumed. The functions ψ_i and ϕ_f are the wave functions describing the target and residual nuclei. From the Schrödinger equations satisfied by ψ_i and ϕ_f, one immediately obtains

$$f_{fi}(\mathbf{r}) \xrightarrow[r\to\infty]{} e^{-\kappa r}/r \tag{5.1}$$

where

$$\frac{2m}{\hbar^2}(E_i - E_f) = \kappa^2 \tag{5.2}$$

The energy $(E_i - E_f)$ equals the energy required to break up the final nucleus into the initial nucleus plus a zero-energy neutron.

The overlap wave function generally used in a stripping DWA calculation is obtained by solving the Schrödinger equation for a neutron moving in the mean field of the target nucleus. The latter is taken to be an empirical potential such as the Woods–Saxon potential [see Bear and Hodgson (78)] whose parameters are appropriate for the target nucleus and the neutron single-particle state under study, and of course satisfy (5.1) and (5.2). This last condition is important to the extent that the reaction occurs at the surface. Harmonic oscillator wave functions are not adequate because they do not satisfy (5.1) and (5.2). Obviously, the more realistic the models used in terms of the experimental evidence that they can explain, the more meaningful is the understanding of nuclear structure that can be extracted from the one-particle transfer reactions.

The overlap wave function is significantly modified when the target and/or the residual nuclei are deformed, since the effects of deformation are most important on the surface region. The deformed potential is obtained from a spherical one that has been found suitable for spherical nuclei in a nearby range of the periodic table. One can, for example, expand the radius parameter R in a multipole series. [See Rost (67) and Bang and Vaagen (80) for details.]

6. THREE-BODY MODEL[‡]

The three bodies in this model are the neutron, the proton, and the target nucleus. The neutron–nucleus and proton–nucleus interactions are taken to be the optical model potentials, while the neutron–proton interaction usually is a simplified version of the nucleon–nucleon interaction, allowing of course for the formation of the deuteron. The optical model potentials include the effects of the excitation of the target nucleus on the elastic scattering of the neutron and proton by the nucleus. Otherwise, the nucleus is inert, so that inelastic and fragmentation processes are not included in this model.

[‡]Austern, Iseri, et al. (87).

The focus of the study of this system is on the effect of breakup on the wave function and on the elastic scattering of the deuteron. The approximations used eliminate the stripping channel. Stripping is calculated in the next order of approximation by using the three-body model wave function in the DWA transition amplitude. The implied assumption is that the stripping channel does not induce a substantial change in the wave function.

The simplest Schrödinger equation for the three-body model has the following form:

$$[E - T_p - T_n - V_{pn} - (V_p + iW_p) - (V_n + iW_n)]\psi(\mathbf{r}_p, \mathbf{r}_n) = 0 \tag{6.1}$$

The quantities T_p and T_n are the kinetic energy operator for the proton and neutron respectively, V_{pn} is the neutron–proton interaction, and $V_p + iW_p$ and $V_n + iW_n$ are optical model potentials. The energy dependence of the empirical optical model parameters present a problem in that the energy at which these parameters should be used is not clear. The practice has been to evaluate them at an energy equal to $E/2$ on the supposition that the neutron and proton share the energy equally, as is approximately the case for the incident deuteron. There is in addition a threshold effect; the absorption potential W_n must go to zero when the proton energy exceeds E, since then the neutron is bound. To take this effect into account, W_n in (6.1) is replaced by

$$W_n \to W\left(\mathbf{r}, \frac{E}{2}\right)\theta(E - h_p) \tag{6.2}$$

where θ is the unit function and h_p is the proton Hamiltonian

$$h_p = T_p + V_p \tag{6.3}$$

A similar modification is suggested for W_p.

One should also take antisymmetry into account. The wave functions of the neutron and proton must be orthogonal to the wave functions of the nucleons in the target nucleus.

In most of the calculations that have been performed, the threshold effect and the antisymmetry are neglected. Estimates of the latter are discussed by Austern. We then return to the Schrödinger equation, (6.1).

We discuss three procedures that have been used to obtain approximate solutions to (6.1). In all of these approximations, the variables

$$\mathbf{r} = \mathbf{r}_p - \mathbf{r}_n \qquad \mathbf{R} = \frac{\mathbf{r}_p + \mathbf{r}_n}{2} \tag{6.4}$$

are used. Letting

$$U \equiv V + iW$$

the potential in (6.1) becomes

$$U_p\left(\mathbf{R}+\frac{\mathbf{r}}{2}\right)+U_n\left(\mathbf{R}-\frac{\mathbf{r}}{2}\right)+V_{np}(\mathbf{r}) \tag{6.5}$$

A Coulomb term $U_C(\mathbf{R})$, dependent on $\mathbf{R}$ only, is added to (6.5). Since the dependence of the Coulomb potential on $\mathbf{r}$ is neglected, this term will have no effect on break up.

A. Watanabe Potential[†]

This is obtained by taking the expectation value of (6.1) with respect to the internal deuteron wave function $\phi_d(\mathbf{r})$, omitting the ${}^3D_1$ state component of ϕ_d. This yields the equation

$$[E+|\varepsilon_d|-T_R-U_C(R)-U_{Wat}(R)]\psi(\mathbf{R})=0 \tag{6.6}$$

where T_R is the kinetic energy of the center of mass of the neutron–proton system,

$$U_{Wat}\equiv\int d\mathbf{r}\,|\phi_d(\mathbf{r})|^2\left[U_p\left(\mathbf{R}+\frac{\mathbf{r}}{2}\right)+\mathbf{U}_n\left(\mathbf{R}-\frac{\mathbf{r}}{2}\right)\right] \tag{6.7}$$

and

$$\psi(\mathbf{r}_p,\mathbf{r}_n)\equiv\Psi(\mathbf{r},\mathbf{R}) \tag{6.8}$$

has been approximated by

$$\Psi(\mathbf{r},\mathbf{R})\simeq\phi_d(\mathbf{r})\Psi(\mathbf{R}) \tag{6.9}$$

The Watanabe potential is just an example of the folding potential [see (V.2.76)]. In view of (6.9), the breakup channel is not included.

B. The Adiabatic Approximation[‡]

We first rewrite (6.1) in the neutron–proton relative and center-of-mass coordinates, $\mathbf{r}$ and R, respectively:

$$(E-h_{np}-T_R-U(\mathbf{r},\mathbf{R}))\psi(\mathbf{r},\mathbf{R})=0 \tag{6.10}$$

[†]Watanabe (58).
[‡]Johnson and Soper (70).

where

$$U(\mathbf{r},\mathbf{R}) \equiv U_p + U_n + U_c$$

and h_{np} is the neutron–proton Hamiltonian

$$h_{np} = T_r + V_{np} \tag{6.11}$$

T_r is the kinetic energy of the relation motion of the neutron and proton. The adiabatic approximation is obtained by replacing h_{np} by $-|\varepsilon_d|$, where ε_d is the binding energy of the deuteron, with the result

$$(E + |\varepsilon_d| - T_R - U(\mathbf{r},\mathbf{R}))\psi^{AD}(\mathbf{r},\mathbf{R}) = 0 \tag{6.12}$$

This equation is solved as a scattering problem in the variable **R**; the variable **r** is taken to be a parameter, so that solutions are calculated for each value of **r**. The incident wave is taken to be $\phi_d(\mathbf{r})e^{i\mathbf{K}\cdot\mathbf{R}}$. Deuteron elastic scattering is obtained by taking the expectation value of the outgoing component of ψ^{AD} with respect to the deuteron wave function $\phi_d(\mathbf{r})$. Breakup is obtained by taking the expectation value with respect to the neutron–proton continuum wave functions, $\phi(\mathbf{k},\mathbf{r})$.

C. Coupled Equations‡

The Watanabe wave function, (6.9), is the first term in a more complete expansion of $\Psi(\mathbf{R},\mathbf{r})$ in terms of the bound state (the deuteron) and the continuum states of two nuclear system. Austern, Iseri, et al. (86) write

$$\begin{aligned}\Psi(\mathbf{r},\mathbf{R}) &= \sum_{JM} a_{JM}\frac{1}{R}\psi_{JM}(\mathbf{r},\mathbf{R})\\ \psi_{JM}(\mathbf{r},\mathbf{R}) &= \phi_D(\mathbf{r})f^J(R)Y_{JM}(\hat{R})\\ &\quad + \sum_l \sum_{L=|J-l|}^{J+l} \int_0^\infty dk\,\phi_l(k,r)g^J_{lL}(\lambda,R)[Y_l(\hat{\mathbf{r}}), Y_L(\hat{\mathbf{R}})]_{JM}\end{aligned} \tag{6.13}$$

In this equation $f^J(R)$ and $g^J_{lL}(\lambda,R)$ are unknown functions to be determined by the coupled equations obtained when (6.13) is substituted for the wave function in the Schrödinger equation. The continuum wave function $\phi_l(k,r)Y_{lm}$ satisfies the neutron–proton equation:

$$\begin{aligned}[\varepsilon(k) - T_r - V_{pn}(r)]\phi_l(k,r)Y_{lm}(\hat{\mathbf{r}}) &= 0\\ \varepsilon(k) &= \frac{\hbar^2k^2}{M}\end{aligned} \tag{6.14}$$

‡Austern, Iseri, et al. (89).

The parameter λ gives the center-of-mass momentum of the neutron–proton system, so that

$$E = \varepsilon(k) + \frac{\hbar^2\lambda^2(k)}{4M} \tag{6.15}$$

Finally, $[Y_l(\hat{\mathbf{r}}),\ Y_L(\hat{\mathbf{R}})]_{JM}$ is given by

$$[Y_l(\hat{\mathbf{r}}),\ Y_L(\hat{\mathbf{R}})]_{JM} = \sum_{m,\mu} \langle JM | lm, L\mu \rangle\, Y_{lm}(\hat{r}) Y_{L\mu}(\hat{R}) \tag{6.16}$$

The first term of (6.13) describes elastic deuteron scattering, and the second term describes the breakup component. The expansion in l permits the description of the effects connected with the orientation of the deuteron.

Inserting (6.13) into the three-body Schrödinger equation leads to an infinite set of coupled differential-integral equations. Some method of truncation is needed. The dynamical origin of the coupling is in the potential U:

$$U = U_p\left(\mathbf{R} + \frac{\mathbf{r}}{2}\right) + U_n\left(\mathbf{R} - \frac{\mathbf{r}}{2}\right) + U_c \tag{6.17}$$

This can be expanded in a *multipole* series:

$$U = \sum_l U_l(r, R) P_l(\hat{\mathbf{r}}\cdot\hat{\mathbf{R}}) \tag{6.18}$$

If $U_p \approx U_n$, which is nearly true, the sum goes over the even l's only. *Truncation of this series at* $l = l_{\max}$ is reasonable physically. A *posteriori* verification can be obtained, and in fact $l_{\max}$ equals 2; that is, only two terms in (6.18) are needed.

This is demonstrated by Table 6.1, which gives the partial cross sections as $l_{\max}$ is increased beyond 2 for $J = 17$, the dominant wave in the example discussed by Austern, Iseri, et al. (87). The $l = 1$ contribution is found to be unimportant.

TABLE 6.1 Partial Cross Section $\sigma_l^{(J)}$ for $J = 17$

$l_{\max}$	2	4	6	0
$\sigma_0^{(17)}$	4.067	3.930	3.989	10.273
$\sigma_2^{(17)}$	12.596	11.651	11.351	
$\sigma_4^{(17)}$		1.830	1.684	
$\sigma_6^{(17)}$			0.202	
$\sum_l \sigma_l^{(J)}$	16.663	17.411	17.226	10.275
$\sigma_{\text{el}}^{(J)}$	74.230	73.502	73.568	90.106
$\sigma_{\text{react}}^{(J)}$	99.444	100.32	100.33	93.429

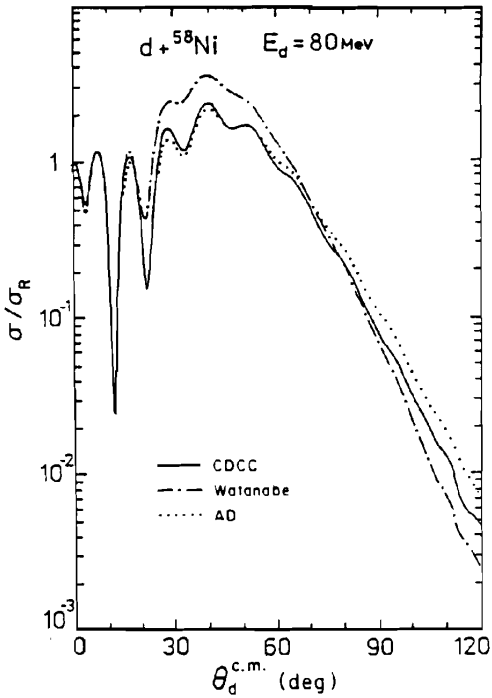

FIG. 6.1. Elastic scattering cross-sections for $d + {}^{58}\text{Ni}$. Comparisons are made between the Watanabe model, the adiabatic approximation, and the coupled-channel (CDCC) calculations [Yahiro (85)]. [From Austern, Iseri, et al. (87).]

We also see that the Watanabe ($l = 0$) term is not usable. To be consistent, one must similarly cut off the expansion over l in (6.13) at l in (6.13) at $l = l_{\max}$. The Schrödinger equation for $\psi(\mathbf{r}, \mathbf{R})$ now becomes a finite set of coupled integrodifferential equations. These must be solved numerically. In making this truncation, the stripping channel asymptotic amplitude vanishes faster than $1/r$, so that this formulation can yield a finite stripping amplitude only in the next approximation, described below.

The Watanabe potential is obtained if only the first term in (6.13) is retained. The adiabatic approximation can be obtained from (6.13) if $\varepsilon(k)$ is appropriately replaced by $-|\varepsilon_d|$, or as is sometimes done, by a constant that can be used as a parameter. Of the three approaches, the coupled-equation description should thus be regarded as the most precise.

The elastic scattering and breakup cross sections calculated using these three approximations are shown in Figs 6.1 and 6.2. From Fig. 6.1 we note that the Watanabe cross section is in substantial disagreement with the coupled-equation results beyond about 30°. The adiabatic cross section is in much better agreement departing from the coupled-equation results at about 90°. On the other hand,

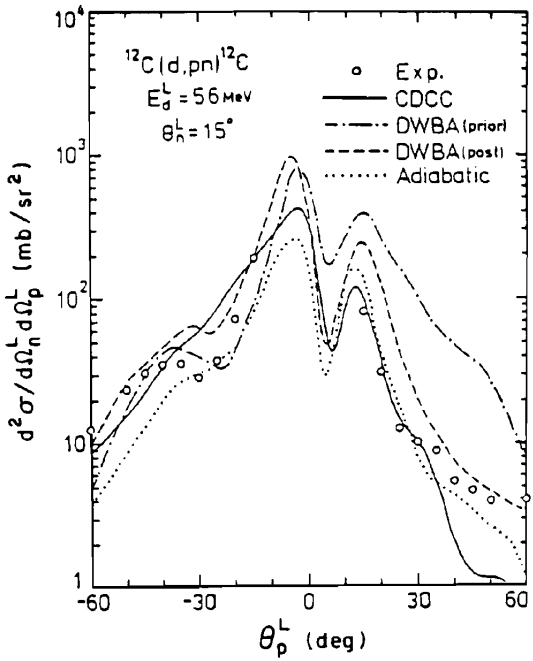

FIG. 6.2. Comparison of breakup cross sections of 56-MeV deuterons by ^{12}C with calculations by CDCC, DWBA, and the adiabatic models. In this experiment the neutron detector is fixed at $\theta_n^L = 15°$ [Yahiro, Iseri, Kamimura, and Makano (84); Yahiro 85)]. (From Austern, Iseri, et al. (87).]

the adiabatic breakup cross section (Fig. 6.2) has a slope similar to that obtained with the coupled equations but fails when the proton angle θ_p^L deviates substantially from the neutron angle θ_n^L.

The importance of the $l = 2$ term for the elastic scattering, which gives rise to the deviation from the Watanabe results, can also be seen when an optical model potential is fitted to the coupled-equation elastic scattering. The Watanabe potential has a very diffuse surface. But according to Austern, Iseri, et al. (87), when the effect of the $l = 2$ multipole is included, the diffusiveness of the optical model potential is reduced to a value equal to that of the nucleon optical model potential. This is in good agreement with the empirical results of Section 4. A similar behavior is found when the adiabatic model is used.

Stripping can be calculated on the basis of the three-body model using the $\mathcal{T}$-matrix element

$$\mathcal{T}_{dp} = \langle \chi_p^{(-)}(\mathbf{k}_p, \mathbf{r}_p)\psi_n(\mathbf{r}_n)V_{pn}\psi^{(+)}(\mathbf{r}_p, \mathbf{r}_n)\rangle \tag{6.19}$$

where the outgoing nucleon is a proton and $\psi^{(+)}(\mathbf{r}_p, \mathbf{r}_n)$ is chosen to be the three-body model eigenfunction corresponding to an incident deuteron. In the

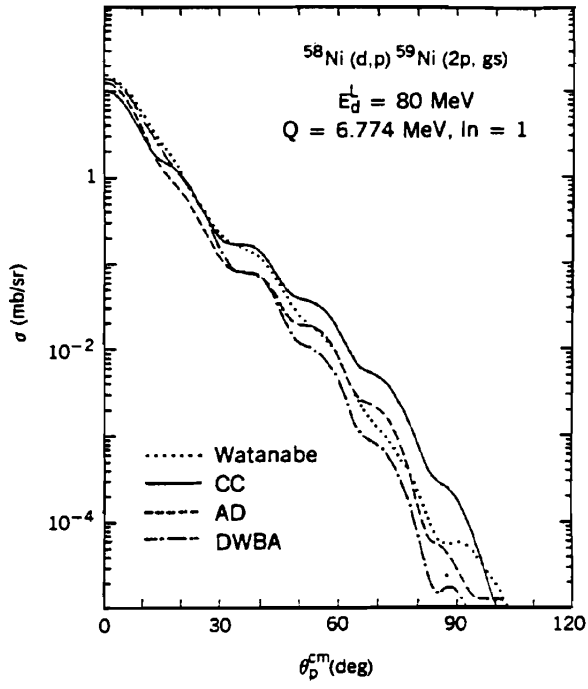

FIG. 6.3. Cross sections for ^{58}Ni(d, p) ^{59}Ni$(3p$, g.s.$)$ at $E_d = 80$ MeV obtained from CDCC, AD, Watanabe, and DWA Calculations [Iseri (85)]. [From Austern, Iseri, et al. (87).]

zero range approximation,

$$(\mathcal{T}_{dp})_{ZR} = \int d\mathbf{R}\chi_p^{(-)*}(\mathbf{R})\psi_n^*(\mathbf{R})\phi^{(+)}(\mathbf{k}_d, \mathbf{R}) \tag{6.20}$$

with

$$\phi^{(+)}(\mathbf{k}_d, \mathbf{R}) = 8\int d\mathbf{r}V_{pn}(\mathbf{r})\Psi^{(+)}(\mathbf{r}, \mathbf{R}) \tag{6.21}$$

Roughly, $\phi^{(+)} \sim \Psi^{(+)}(0, \mathbf{R})$.

We now look for the effects on stripping of the break up channels. These are two in number. First the presence of the breakup channels will draw flux, so that the contribution of the $\phi_D f^J(r)$ term in (6.13), to be referred to as the *elastic* contribution, will be reduced. Second, in the event of poor momentum matching, thereby reducing the elastic contribution (see p. 482), the breakup contribution may become important since there will be a range in k in the breakup component of (6.13) which permits good momentum matching.

These effects are illustrated in Figs 6.3 to 6.5. In Fig. 6.3 we compare the calculations using the deuteron wave function provided by the Watanabe

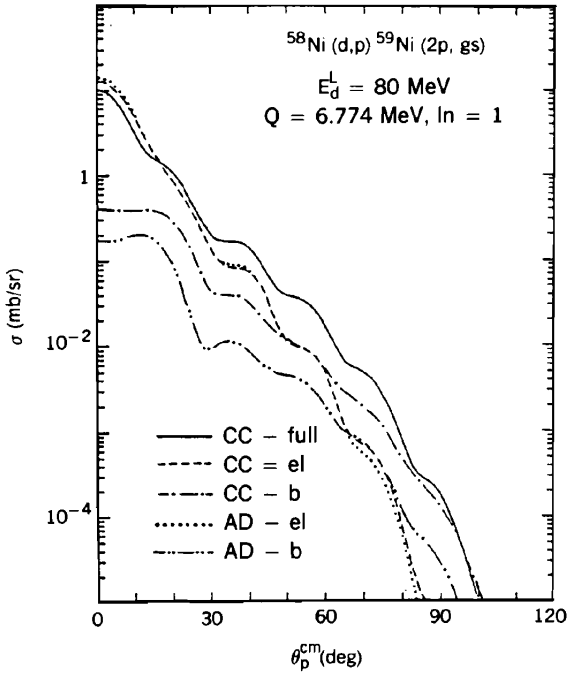
^{58}Ni (d,p) ^{59}Ni (2p, gs)
E_d^L = 80 MeV
Q = 6.774 MeV, ln = 1
CC – full
CC – el
CC – b
AD – el
AD – b
σ (mb/sr)
θ_p^{cm}(deg)

FIG. 6.4

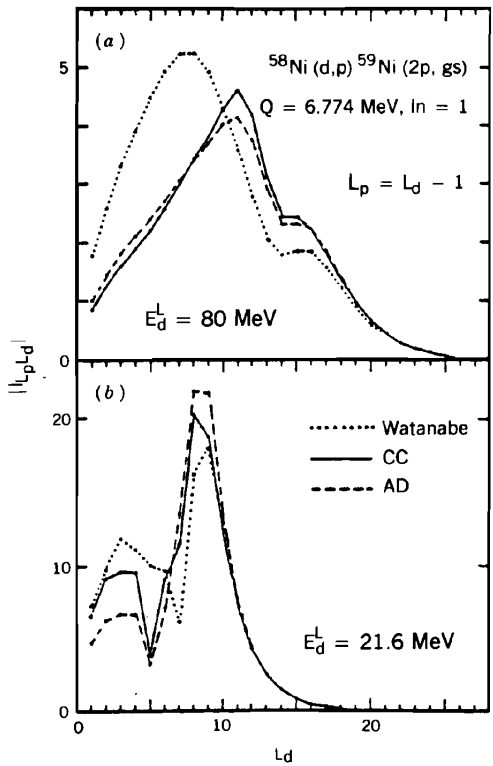
(a)
^{58}Ni (d,p) ^{59}Ni (2p, gs)
Q = 6.774 MeV, ln = 1
$L_p = L_d - 1$
E_d^L = 80 MeV
(b)
Watanabe
CC
AD
E_d^L = 21.6 MeV
L_d

FIG. 6.5

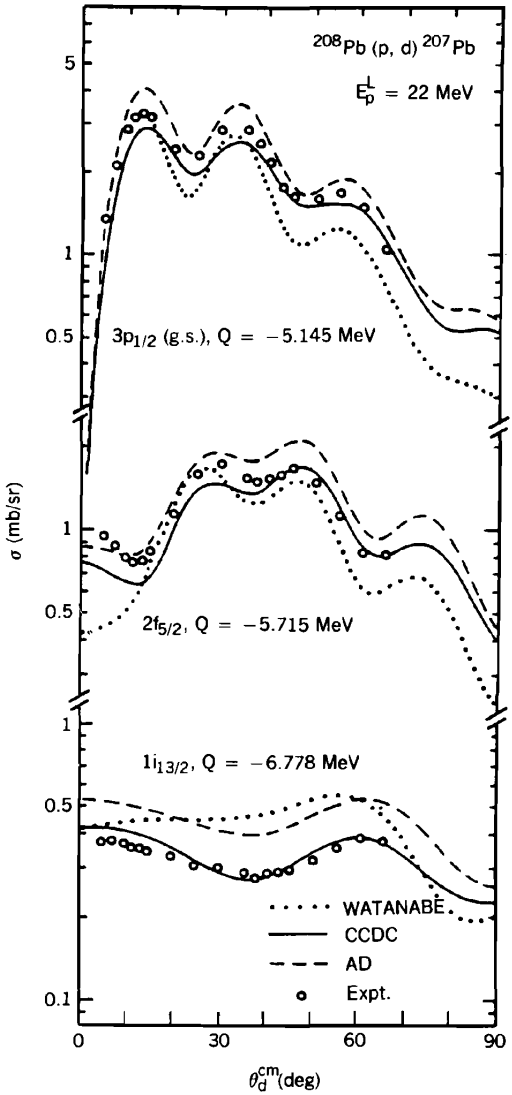

FIG. 6.6. Cross section for the reaction ^{208}Pb (p, d) at $E_p = 22$ MeV. The incident protons are polarized [Iseri (85)]. (From Austern Iseri, et al. (87).]

FIG. 6.4. Decomposed cross sections for ^{58}Ni(d, p) ^{59}Ni$(2p, \text{g.s.})$ at $E_d = 80$ MeV for the CDCC and AD calculations showing the contributions for the elastic and breakup processes [Iseri (85)]. [From Austern, Iseri, et al. (87).]

FIG. 6.5. Modulus of the overlap integral I for ^{58}Ni (d, p) ^{59}Ni $(2p, \text{g.s.})$ at $E_d = 80$ and 21.6 MeV. The angular momentum L_p is taken to equal $L_d - 1$ [Iseri (85)]. [From Austern, Iseri, et al. (87).]

potential, the adiabatic approximation, the coupled-equation procedure, and the DWA. In the last case, a deuteron potential that yields a coupled-equation elastic cross section. Comparison of the coupled equation with the Watanabe result demonstrates the importance of breakup, especially at the larger angle. The adiabatic cross section and the DWA also disagree with the coupled-equation results. In the former case, which includes breakup, the deviation from the coupled equation results is presumably due to the inaccuracy in the breakup amplitude because of the adiabatic assumption. Phase relations are extremely important in this situation. But in addition, the adiabatic approximation includes only the $l = 0$ breakup contribution not the $l = 2$. This effect in important at lower energies.

Further insight is obtained from Fig. 6.4 in which are plotted the elastic and breakup contributions to the stripping cross sections for both the adiabatic and coupled-equation approximations. In the coupled-equation case, note that the breakup contribution dominates beyond proton angles of 50°. In the adiabatic case this crossover does not occur. In fact, the breakup cross section is much smaller than the elastic cross section over the entire angular range. Figure 6.5 demonstrates that breakup reduces the contribution to stripping made by the smaller deuteron angular momenta in the Watanabe calculation. Breakup thereby emphasizes the surface character of stripping.

In Fig. 6.6 the three methods are compared with experimental data. We see that in these cases, by far the best results are achieved with coupled equations. The adiabatic approximation is a considerable improvement over the Watanabe recipe, especially at large angles.

In conclusion, the single-step DWA approximation of Section 3 can be considered to be valid only in the forward angular range. Employing the adiabatic model will result in a substantial improvement. But the use of the more exact coupled-equation method is computationally laborious, limiting its utilization for the analysis of data.